TURBULENT DIFFUSION IN ROUND TUBES

J. A. Zwolinski, et al

Army Mobility Equipment Research and
Development Center
Fort Belvoir, Virginia

February 1973

DISCLAIMER NOTICE

THIS DOCUMENT IS BEST QUALITY PRACTICABLE. THE COPY FURNISHED TO DTIC CONTAINED A SIGNIFICANT NUMBER OF PAGES WHICH DO NOT REPRODUCE LEGIBLY.

AD

Report 2053

TURBULENT DIFFUSION IN ROUND TUBES

by

J. A. Zwolinski
S. W. Chi
A. S. Patil

February 1973

Approved for public release; distribution unlimited.

U. S. ARMY MOBILITY EQUIPMENT RESEARCH AND DEVELOPMENT CENTER
FORT BELVOIR, VIRGINIA

AD

Report 2053

TURBULENT DIFFUSION IN ROUND TUBES

by

J. A. Zwolinski
S. W. Chi
A. S. Patil

February 1973

U. S. ARMY MOBILITY EQUIPMENT RESEARCH AND DEVELOPMENT CENTER
FORT BELVOIR, VIRGINIA

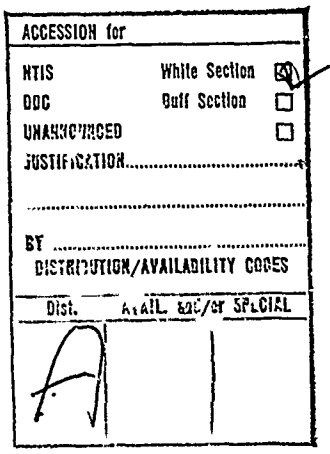

Destroy this report when no longer needed.
Do not return it to the originator.

The citation in this report of trade names of commercially available products does not constitute official endorsement or approval of the use of such products.

UNCLASSIFIED

Security Classification

DOCUMENT CONTROL DATA - R & D

(Security classification of title, body of abstract and indexing annotation must be entered when the overall report is classified)

1. ORIGINATING ACTIVITY (Corporate author)	2a. REPORT SECURITY CLASSIFICATION
Mechanical Technology Department U. S. Army Mobility Equipment Research and Development Center Fort Belvoir, Virginia 22060	Unclassified 2b. GROUP

3. REPORT TITLE

TURBULENT DIFFUSION IN ROUND TUBES

4. DESCRIPTIVE NOTES (Type of report and inclusive dates)

Interim Report Sept 1971 – June 1972

5. AUTHOR(S) (First name, middle initial, last name)

J. A. Zwolinski
S. W. Chi
A. S. Patil

6. REPORT DATE	7a. TOTAL NO. OF PAGES	7b. NO. OF REFS
February 1973	64	18

8a. CONTRACT OR GRANT NO.	9a. ORIGINATOR'S REPORT NUMBER(S)
b. PROJECT NO. 1T061101A91A	2053
c. Task 087	9b. OTHER REPORT NO(S) (Any other numbers that may be assigned this report)
d.	

10. DISTRIBUTION STATEMENT

Approved for public release; distribution unlimited.

11. SUPPLEMENTARY NOTES	12. SPONSORING MILITARY ACTIVITY
	USAMERDC In-House Research Fort Belvoir, Virginia 22060

13. ABSTRACT

Fully developed turbulent flow of air at Re = 1.5 x 10^4 to 3 x 10^4 entered a porous tube with circular cross section. Helium and air were injected uniformly through the tube wall for 36 radii at various ratios of mass velocity through the tube wall to the average mass velocity at the entrance cross section of the tube ranging from 0.0001 to 0.0004. Measurements of the velocity field were made for air injection, and measurements of helium concentration were made for helium injection. Within the tested range of air injection, the distortion of the fully developed velocity profile in terms of $u/\bar{u}$ is negligible.

The numerical solution of diffusion equation was obtained based upon the assumption that the nondimensional velocity distribution, $u/\bar{u}$, was a function of the entrance Reynolds number but independent of small wall-mass injection rates. Prandtl mixing length theory incorporating Van Driest's damping factor generalized by Kinney and Sparrow for the case of wall-mass transfer was used to evaluate effective diffusivity for turbulent flow. The accuracy of the present theory was compared with Kays' correlation of turbulent heat transfer data with zero mass injection, Raithby's exact solution of laminar heat transfer with and without wall-mass transfer, and the present experiments of turbulent diffusion. Excellent agreement with present theory is obtained in all these comparisons.

For convenience of users of the present theory, complete computer listing with users' instruction is appended to the report. The results are pertinent to reverse osmosis desalination processes, water supply systems, catalytic converters for pollutant control, and the numerous subject areas in which a mixing of gases is predominant.

DD FORM 1 NOV 68 1473 REPLACES DD FORM 1473, 1 JAN 64, WHICH IS OBSOLETE FOR ARMY USE.

63

UNCLASSIFIED

Security Classification

14 KEY WORDS	LINK A		LINK B		LINK C	
	ROLE	WT	ROLE	WT	ROLE	WT
Diffusion						
Heat and Mass Transfer						
Evaporation						
Absorption						
Simulation						
Turbulent Boundary Layer						
Laminar Boundary Layer						
Injection of Gases						
Computer Programs						

10 54

1 3-4 47,463—Ft Belvoir

U. S. ARMY MOBILITY EQUIPMENT
RESEARCH AND DEVELOPMENT CENTER
FORT BELVOIR, VIRGINIA

Report 2053

TURBULENT DIFFUSION IN ROUND TUBES

Task 1T061101A91A00

February 1973

Distributed by

The Commander
U S. Army Mobility Equipment Research and Development Center

Prepared by

J. A. Zwolinski
S. W. Chi
A. S. Patil
Independent Laboratory In-House Research
Mechanical Technology Department

ib

SUMMARY

Experiments were performed with fully developed turbulent flows of air at Re = 1.5×10^4 to 3×10^4 entering a porous tube with circular cross section. Helium and air were injected uniformly through the tube wall for 36 radii at various ratios of mass velocity through the tube wall to the average mass velocity at the entrance cross section of the tube ranging from 0.0001 to 0.0004. Measurements of velocity field were made for the case of air injection, and measurements of helium concentration were made for the case of helium injection. Within the tested range of air injection, the distortion of the fully developed velocity profile in terms of $u/\bar{u}$ is negligible.

Numerical solution of the diffusion equation was obtained based upon the assumption that the nondimensional velocity distribution, $u/\bar{u}$, was a function of the entrance Reynolds number but independent of small wall-mass injection rates. Prandtl mixing length theory incorporating Van Driest's damping factor generalized by Kinney and Sparrow for wall-mass transfer was used to evaluate effective diffusivity for turbulent flow. Accuracy of the present theory was compared with Kays' correlation of turbulent heat transfer data with zero mass injection, Raithby's exact solution of laminar heat transfer with and without wall-mass transfer, and the present experiments of turbulent diffusion. Excellent agreement with present theory was obtained in all these comparisons.

For the convenience of users of the present theory, a complete computer listing with users' instruction is appended to the report. The results are pertinent to reverse osmosis desalination processes, water supply systems, catalytic converters for pollutant control, and the numerous subject areas in which a mixing of gases is predominant.

FOREWORD

The present study was performed between 1 September 1971 and 1 June 1972 during the authors' association with USAMERDC's Independent Laboratory In-House Research program sponsored by the Technical Director. The research effort was conducted under Project 1T061101A91A, Task Area 00 087EF.

The authors are particularly grateful to Mr. William B. Taylor, Technical Director, and Mr. Donald B. Dinger, Associate Deputy for Research and Development, USAMERDC, for their monetary support and encouragement. Further, the authors acknowledge the direct help of the supporting facilities within USAMERDC (i.e., the metal, wood, plastics, and painting shops) for their excellent performance in the construction of the laboratory and test equipments. The authors also acknowledge the efforts of their direct-line supervisory personnel for their special handling of this program: Mr. J. H. Yeardley, Chief, Construction Equipment Division; Mr. J. K. Knaell, Chief, Materials Handling Equipment Development Branch; Mr. A. J. Rutherford, Chief, Mechanical Equipment Division; and Mr. M. H. Henderson, Chief, Mechanical Technology Department.

CONTENTS

Section	Title	Page
	SUMMARY	ii
	FOREWORD	iii
	NOMENCLATURE	v
	ILLUSTRATIONS	vii
I	INTRODUCTION	
	1. The Problem Investigated	1
	2. Review of Present State of Knowledge	2
	3. Purpose and Scope of Present Work	3
II	EXPERIMENTS	
	4. Apparatus and Instrumentation	3
	5. Test Procedure and Measurements	8
	6. Test Results	8
III	THEORETICAL DEVELOPMENT	
	7. Theoretical Model	13
	8. Solution of Diffusion Equation by Finite Difference	18
IV	RESULTS AND DISCUSSION	
	9. Summary of Results	23
	10. Accuracy of Calculation Scheme	23
	11. Justification of Main Assumption and Comparison with Experiments	29
V	CONCLUSIONS	
	12. Conclusions	36
	APPENDICES	
	A. Entrance Velocity Profile, $\phi_o(\eta)$	38
	B. Listing and Users' Instruction of Computer Program for Turbulent Diffusion in Round Tubes	40

NOMENCLATURE

A	constant equal to 26 in Van Driest's damping factor, Equation (13)
A_j, B_j	coefficients, Equations (28) and (29)
A_o, B_o	coefficients A_j, B_j at j=o, Equations (36) and (37)
D	laminar diffusivity, Equation (4)
D_e	effective diffusivity for turbulent flow, Equation (1)
$\bar{D}_e$	nondimensional effective diffusivity for turbulent flow, Equation (14)
DF	damping factor, Equation (12)
f	helium mass concentration, Equation (1)
i	superscript indicates grid position in nondimensional axial direction, Equation (21)
j	subscript indicates grid position in nondimensional radial direction, Equation (22)
l	mixing length for turbulent flow, Equation (11)
m	total number of grid points in axial direction, Equation (21)
$\dot{m}''_w$	wall mass flux per unit area and time, Equation (4)
$\bar{m}$	ratio of wall-mass flux per unit area and time to the average mainstream air mass per unit area and time at entrance to porous tube, Equation (6)
n	total number of grid points in radial direction, Equation (22)
Pr	laminar Prandtl number, paragraph 10 of text
r	coordinates in radial direction, Equation (1)
R	tube radius, Fig. 14
R^+	nondimensional R defined as $R\sqrt{\rho\tau_s/\mu}$, Equation (14)
Re	Reynolds number defined as $2R\rho\bar{u}_o/\mu$, Equation (A9)
Re_w	Reynolds number defined as $2R\rho v_w/\mu$, Fig. 20
Sc	laminar Schmidt number, Equation (10)
Sc_t	turbulent Schmidt number equal to 0 · 86, Equation (10)

u	velocity in axial direction, Equation (1)
$\bar{u}$	average axial velocity, Equation (5)
U	nondimensional axial velocity defined by Equation (19)
$\bar{u}_o$	average axial velocity at entrance to porous tube, Equation (6)
u^+	nondimensional u defined as $u/\sqrt{\tau_w/\rho}$, Equation (A6)
$\bar{u}_o^+$	nondimensional u_o defined as $u_o/\sqrt{\tau_w/\rho}$, Equation (A8)
v	velocity in radial direction, Equation (1)
V	nondimensional radial velocity defined by Equation (20)
x	coordinates in axial direction, Equation (1)
$\alpha\beta\gamma\delta$	coefficients defined by Equations (24) through (27)
η	nondimensional coordinates defined as r/R, Equation (5)
$\Delta\eta$	finite increment in η, Equation (22)
μ	laminar dynamic viscosity, Equation (10)
μ_e	effective dynamic viscosity for turbulent flow, Equation (A2)
μ_t	turbulent dynamic viscosity, Equation (10)
ξ	nondimensional coordinates in axial direction defined as x/R, Equation (15)
$\Delta\xi$	finite increment in ξ, Equation (21)
ρ	mixture density assumed constant, Equation (1)
τ	shear stress, Equation (A1)
τ_w	shear stress at tube wall, Equation (A1)
X	nondimensional quantity defined as $\bar{m}Re\,(1-\eta)/4$, Equation (13)

ILLUSTRATIONS

Figure	Title	Page
1	Diagrammatic Representation of the General Problem of Heat and Mass Transfer in Round Tubes	1
2	Layout of the Diffusion Apparatus	3
3	Schematic Representation of the Flow System	4
4	Calibration of the Lintronic Anemometer	5
5	Calibration of the GOW-MAC Gas Analyzer for Helium in Air	6
6	Traversing Mechanism with Gas Analyzer	7
7	Traversing Mechanism with Anemometer	7
8	Measured Turbulent Velocity Profiles at $Re = 1.5 \times 10^4$: X, $\overline{m} = 0$; O, $\overline{m} = -0.0004$	
9	Measured Helium Concentration at $Re = 1.5 \times 10^4$, and $\overline{m} = -0.0002$: X, x/D = 15; O, x/D = 10; Δ, x/D = 5	10
10	Measured Helium Concentration at $Re = 1.5 \times 10^4$, $\overline{m} = -0.0004$: X, x/D = 15; O, x/D = 10	11
11	Measured Helium Concentration at $Re = 3 \times 10^4$ and $m = -0.0001$: X, x/D = 15; O, x/D = 10; Δ, x/D = 5	12
12	Nomenclature for Flow Through a Porous Tube with Injection	13
13	Reynolds Number, Re, Versus Nondimensional Tube Radius, R^+	16
14	Calculated Velocity Profile at $Re = 2 \times 10^3$ to 1×10^6	17
15	Calculated Helium Concentration Profiles at $Re = 5 \times 10^3$ and $\overline{m} = -0.001$	24
16	Calculated Helium Concentration Profiles at $Re = 5 \times 10^4$ and $\overline{m} = -0.001$	25
17	Calculated Helium Concentration Profiles at $Re = 1 \times 10^5$ and $\overline{m} = 0.001$	26

ILLUSTRATIONS (cont'd)

Figure	Title	Page
18	Comparison of Temperature Profiles for Laminar Flow with Constant Heat Flux and Uniform Wall Injection: —, Exact Solution from Raithby; X, Present Theory	27
19	Comparison of Nusselt Number for Laminar Flow with Constant Heat Flux: —, Exact Solution from Raithby, X, Present Theory	28
20	Comparison of Nusselt Number for Fully Developed Turbulent Flow with Constant Heat Flux: —, Kays' Correlation; X, Present Theory	30
21	Comparison of Nusselt Number for Turbulent Flow with Constant Heat Flux: —, Kays' Correlation; X, Present Theory	31
22	Comparison of Calculated and Measured Velocity Profiles at $Re = 1.5 \times 10^4$: —, Present Theory; X, Experiments at $\overline{m} = 0$; O, Experiments at $\overline{m} = -0.0004$	32
23	Comparison of Calculated and Measured Helium Concentration at $Re = 1.5 \times 10^4$ and $\overline{m} = -0.0002$: —, Present Theory; X, O, and Δ, Experiments at x/D = 15, 10, and 5	33
24	Comparison of Calculated and Measured Helium Concentration at $Re = 1.5 \times 10^4$ and $\overline{m} = -0.0004$: —, Present Theory; X and O, Experiments at x/D = 15 and 10	34
25	Comparison of Calculated and Measured Helium Concentration at $Re = 3 \times 10^4$ and $\overline{m} = -0.0001$: —, Present Theory; X, O, and Δ, Experiments at x/D = 15, 10, and 5	35

TURBULENT DIFFUSION IN ROUND TUBES

I. INTRODUCTION

1. The Problem Investigated. Figure 1 illustrates a porous tube with a mainstream of gas flowing in the axial direction. Another gas may flow through the pores in the tube surface to join the mainstream. In addition, liquid droplets may be injected into the gas stream. The flow in the tube is turbulent. Large property variations may exist in the fluid as a result of one or more of the following influences: (1) temperature differences existing between the surface, the mainstream, the secondary stream, and the liquid droplets; (2) composition differences between the different fluids; and (3) chemical reactions between one or more of the fluids.

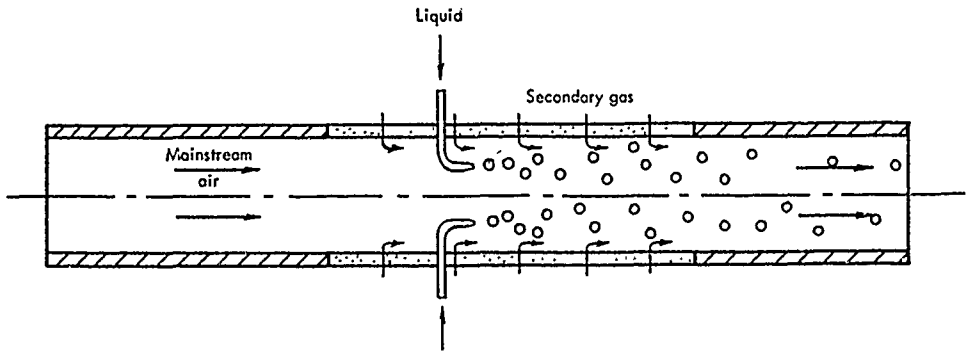

Fig. 1. Diagrammatic representation of the general problem of heat and mass transfer in round tubes.

The flow represented in Fig. 1. contains features which are present, though not usually simultaneously, in a great many circumstances of practical importance. If only one fluid is present (no injection of liquid droplets or secondary gas), the situation is the familiar one of turbulent tube flow; it arises in heat exchangers and numerous other engineering devices. Injection or suction of fluid through the porous tube wall occurs in transpiration cooling of the wall of gas-turbine combustors and reverse-osmosis desalination of saline water; injection may also be resorted to as a means to prevent boundary-layer separation (e.g., to improve efficiency of compressor diffusers). A chemical reaction exists between the secondary and mainstreams in automobile afterburners and catalytic converters for pollutant control. Interaction between liquid droplets and the gas stream occurs in such practical processes as evaporation of water droplets in

humidifiers, absorption of toxic gas by liquid droplets in environmental control equipments, and combustion of fuel droplets in various thermal power units.

The ultimate aims of the present program at USAMERDC are the provision of a theory for the prediction of heat, mass, and momentum transfer in situations such as those of Fig. 1 and applications of the theory to optimize performance of a variety of mobility equipments. However, the first-year investigations reported herein have been concentrated mainly on turbulent diffusion in round tubes. These results are pertinent to automobile afterburners, catalytic converters, reverse osmosis desalination systems, and water-supply systems.

2. **Review of Present State of Knowledge.** Whereas numerous analytical solutions have been obtained for Laminar diffusion,[1-5] limited analyses have been made for turbulent diffusion in tubes. These included an analysis of salt diffusion in water by the method of analogy between momentum and mass transfer,[6] and an analysis of the fully developed concentration profiles.[7] Analyses for the development of concentration profiles for turbulent tube flow have not yet been made.

Tests for turbulent velocity and temperature distributions have been made by Weissberg and Berman[8], Yuan and Galowin[9], Olson and Eckert[10], and many others. A good review is found in Olson and Eckert's paper[11]. No known experimental results for concentration distribution in tubes have been reported.

---

[1]G. Raithby, "Laminar Heat Transfer in the Thermal Entrance Region of Circular Tubes and Two-Dimensional Rectangular Ducts with Wall Suction and Injection," *Int. J. Heat Mass Transfer*, Vol. 14, pp. 223-243 (1971).

[2]U. Merten, H. K. Lonsdale, and R. L. Riley, "Boundary Layer Effects in Reverse Osmosis," *Ind. Eng. Chem. Fundamentals*, Vol. 3, No. 3, pp. 210-213 (1964).

[3]T. K. Sherwood, P. L. T. Brian, R. E. Fisher, and L. Dresner, "Salt Concentration at Phase Boundaries in Desalination by Reverse Osmosis," *Ind. Eng. Chem. Fundamentals*, Vol. 4, No. 2, pp. 113-118 (1965).

[4]W. N. Gill, C. Tieu, and D. W. Zeh, "Concentration Polarization Effects in a Reverse Osmosis System," *Ind. Eng. Chem. Fundamentals*, Vol. 4, No. 4, pp. 433-439 (1965).

[5]S. Srinivasan, C. Tieu, and W. N. Gill, "Simultaneous Development of Velocity and Concentration Profiles in Reverse Osmosis Systems," *Chem. Eng. Sci.*, Vol. 22, pp. 417-433 (1967).

[6]T. K. Sherwood, P. L. T. Brian, R. E. Fisher, and L. Dresner, "Salt Concentration at Phase Boundaries in Desalination by Reverse Osmosis, *Ind. Eng. Chem. Fundamentals*, Vol. 4, No. 2, pp. 113-118 (1965).

[7]R. B. Kinney and E. M. Sparrow, "Turbulent Flow, Heat Transfer, and Mass Transfer in a Tube with Surface Suction," ASME Paper No. 69-HT-4 (1969).

[8]H. L. Weissberg and A. S. Berman, "Velocity and Pressure Distribution in Turbulent Pipe Flow with Uniform Suction," Proceedings, Heat Transfer and Fluid Mechanics Institute (1955).

[9]S. W. Yuan and L. S. Galowin, "Transpiration Cooling in the Turbulent Flow Through a Porous-Wall Pipe," 6th Int. Cong. Appl. Mech., Vol. 2, p. 331 (1957).

[10]R. M. Olson and E. R. G. Eckert, "Experimental Studies of Turbulent Flow in a Porous Circular Tube with Uniform Fluid Injection Through the Tube Wall," *J. Appl. Mech.*, Vol. 33, pp. 7-17 (1966).

[11]*Ibid.*

It may be concluded from the above review that knowledge of turbulent diffusion in tubes had been defective because drastic assumptions are made in theoretical analyses and no experiments are available to verify the theory.

3. **Purpose and Scope of Present Work.** This work is intended to remedy the above defects. For this purpose, experimental data have been obtained for turbulent diffusion of helium in a round tube, a theoretical model has been developed for calculation of turbulent diffusions in round tubes, and confidence in the present theoretical model has been established by comparison with the experiments.

Descriptions of the experiments and theoretical development are given in Sections II and III. Section IV is devoted to a discussion of the results. Conclusions for applications of the present theory are described in Section V. For the convenience of the users of the present theory, a complete listing of the computer program for the present theory is appended to this report.

II. EXPERIMENTS

4. **Apparatus and Instrumentation.** The apparatus used for the experiments consisted of a flow circuit, an air blower, a hot film anemometer system, a gas analyzer system, a traversing mechanism, and a metered helium supply (Fig. 2).

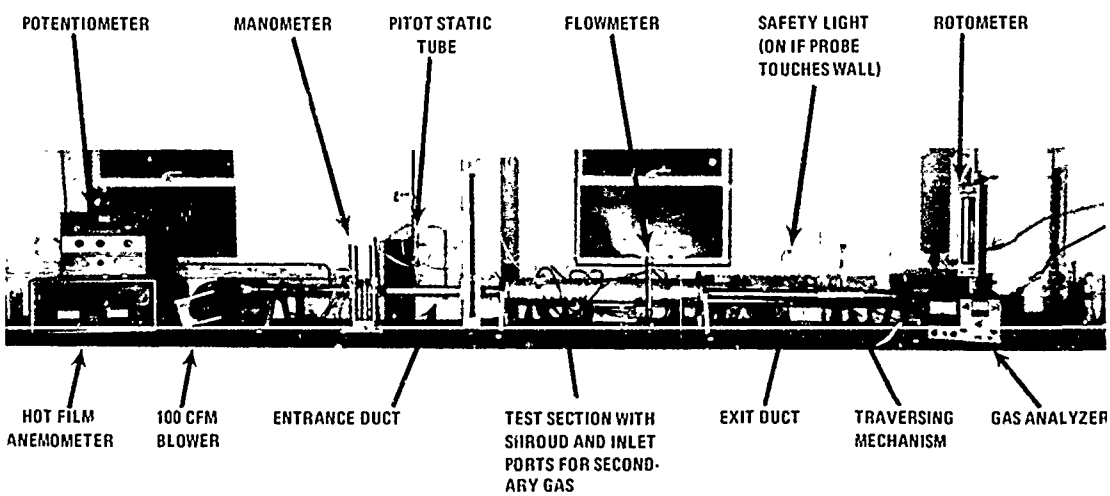

Fig. 2. Layout of the diffusion apparatus.

a. **Flow Circuit and Blower.** A schematic diagram of the flow system is shown in Fig. 3. Air was supplied from a pressure blower with its flow rate controlled by a gate valve upstream of the blower. Downstream of the blower is an entrance tube 1.875 inches ID and 6 feet long followed by a porous test tube 1.875 inches ID and 3 feet long. A traversing mechanism was mounted at the downstream end of the test tube; a description of the traversing mechanism is given in paragraph 4d.

Secondary gas helium, metered by an SK Rotameter, was first introduced into a shroud which surrounds the test tube and then injected into the mainstream air through the porous wall of the test tube. The shroud was filled loosely with fiberglass to insure pressure uniformity. Fine grade (5-μ pore size) sintered stainless steel test tube supplied by Pall Trincor Corporation was used for wall smoothness. Because of the longitudinal pressure drop inside the porous tube with axial flow through it, the radial pressure drop through the tube wall itself should be large so that the radial injection will be uniform along its length. Sintered stainless steel tube is too permeable to insure this; 20 layers of rayon cloth were wrapped around the porous tube. With this combination, a pressure differential of about 2 psi is produced at a radial helium flow rate of 1 SCFM/sq ft.

The above described flow system enabled tests to be conducted with a fully developed turbulent flow of air in a smooth tube entering into a porous tube (36 diameter long) at Re = 1.5×10^4 to 3×10^4 with uniform helium injection along the porous tube.

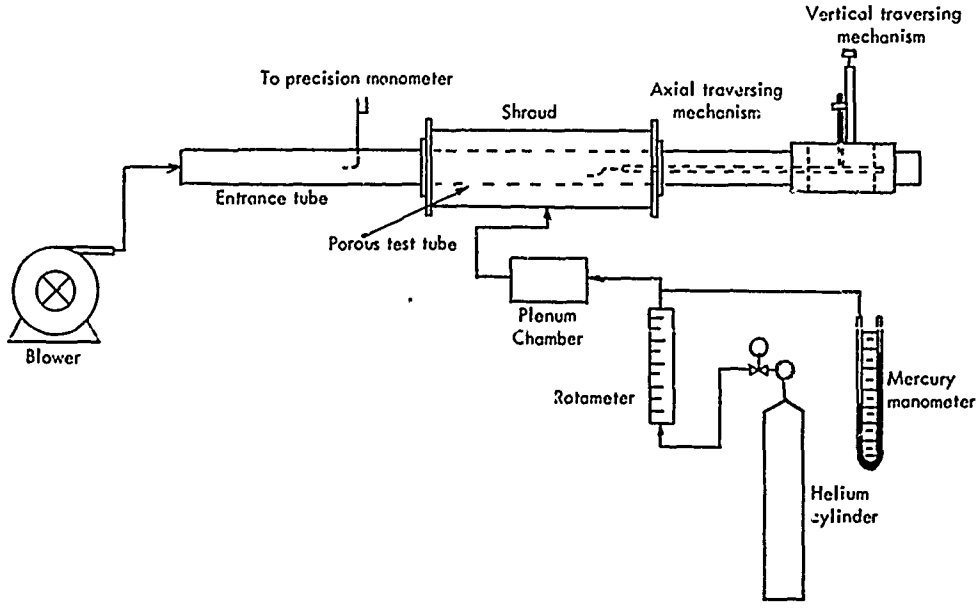

Fig. 3. Schematic representation of the flow system.

b. **Hot-Film Anemometer System.** A hot-film anemometer system purchased from Lintronic Laboratories was used to measure the velocity distributions for turbulent flow. The system consisted of a standard wedge probe and a linear hot-film anemometer with its output monitored by a 10-v d.c. digital voltmeter.

The probe stem was 2 mm in diameter. The sensing element was 1 mm long and 0.2 mm across, and the wedge angle was 8 degrees. The length of the sensing element was set normal to the tube axis. The probe was connected to the Lintronic Constant Temperature Anemometer (Model 40B).

The air velocity and system output voltage relation was linear. A typical linear calibration curve is shown in Fig. 4. The calibration was performed by a standard Aero-Lab pitot-static tube and an NIL precision manometer reading to the nearest 0.001 inch.

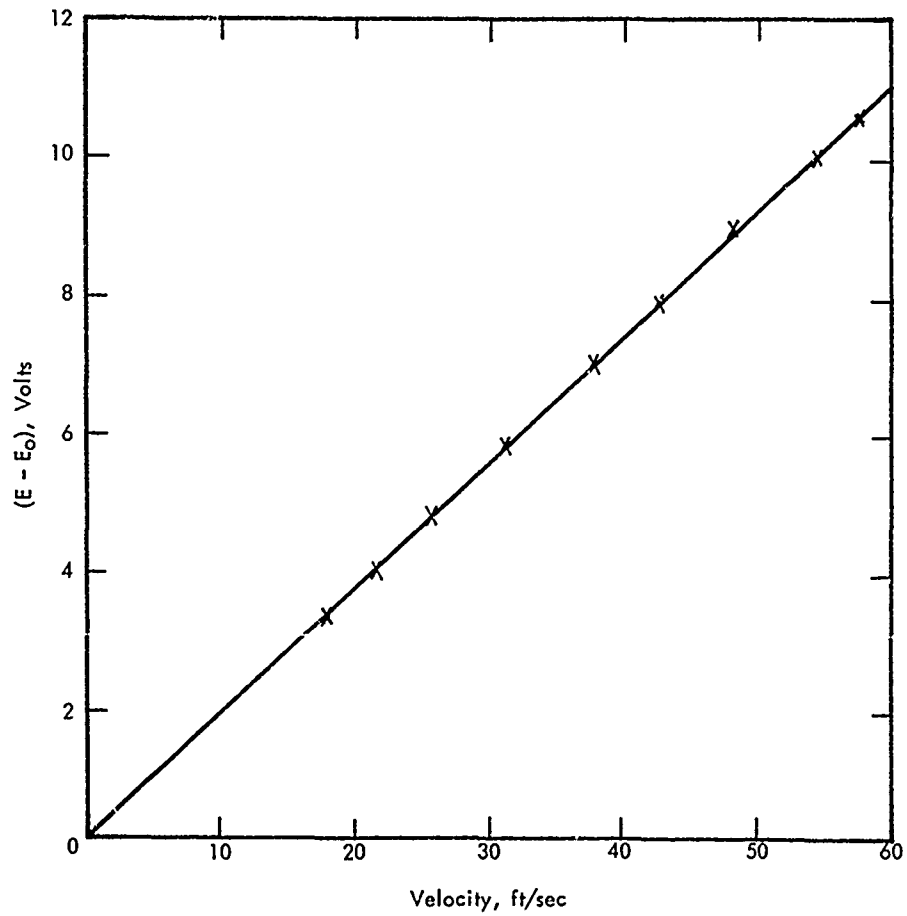

Fig. 4. Calibration of the Lintronic anemometer.

c. **Gas Analyzer System.** A GOW-MAC Model 20-150 thermal conductivity Analyzer, with a diffusion-type thermal conductivity cell, was used to measure helium concentration. The cell contained a sample and reference gas flow geometry. Two detector elements, which formed an electrical Wheatstone bridge circuit and were heated by an electrical current from a constant voltage d.c. power source, were installed in each flow system.

The instrument was balanced by passing reference gas (air) through both the sample and reference flow systems. When a sample gas of different composition was introduced into the sample system, a change in the rate of heat loss occurred caus ing the Wheatstone bridge to unbalance. The output voltage from the detector cell was fed into an analog readout. The instrument was calibrated by a standard helium/air mixture. Figure 5 shows a typical calibration of helium concentration versus analog readout.

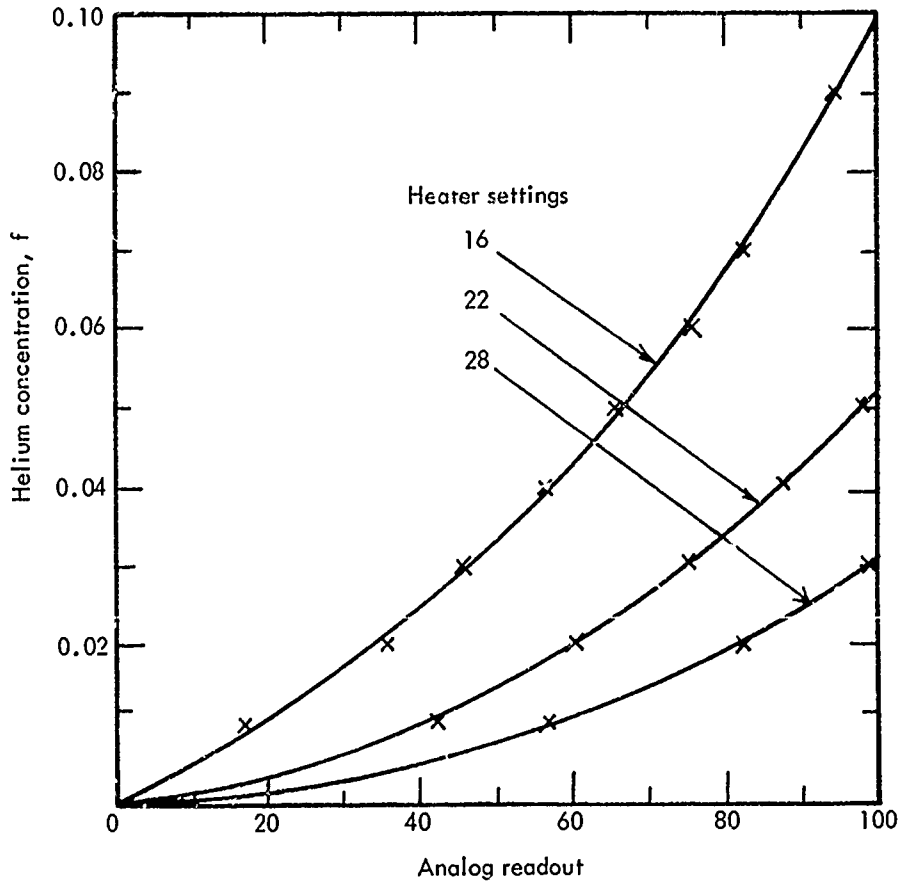

Fig. 5. Calibration of the GOW-MAC gas analyzer for helium in air.

d. Traversing Mechanism. Figure 6 shows the traversing mechanism on which a gas sampling probe was mounted. The gas sampling probe was replaced by a hot-film probe when velocity measurements were made. Figure 7 shows the hot-film probe laid between the traversing mechanism and the Lintronic anemometer.

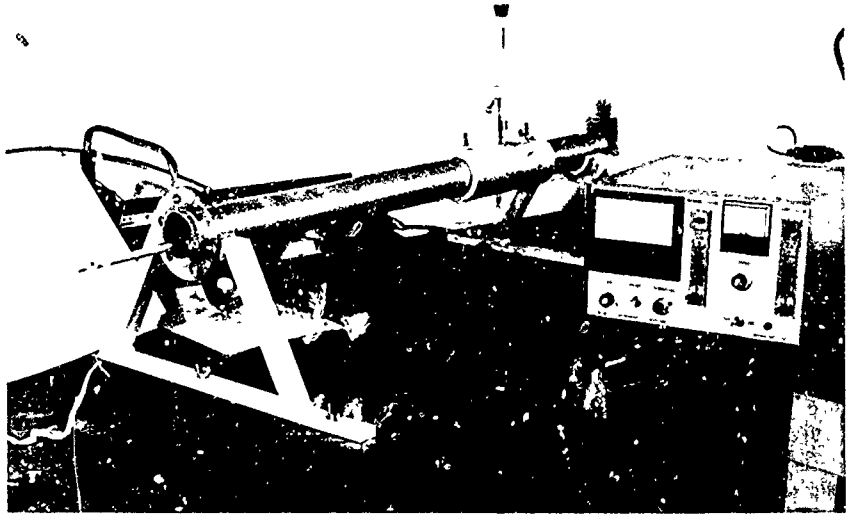

V5219

Fig. 6. Traversing mechanism with gas analyzer.

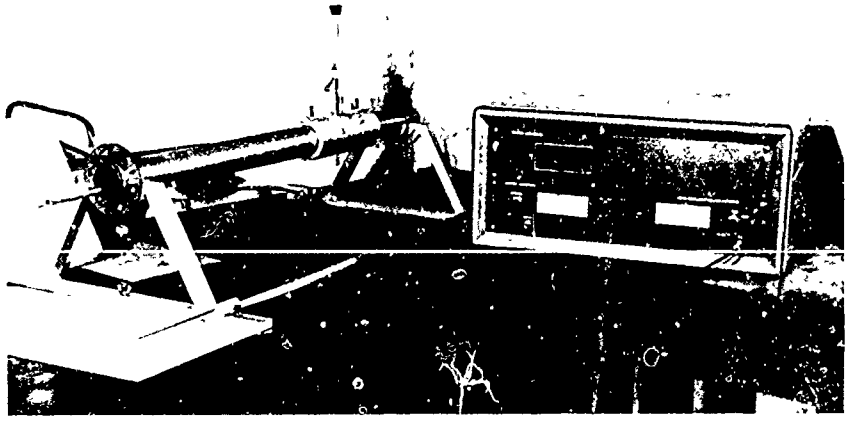

V5215

Fig. 7. Traversing mechanism with anemometer.

The traversing mechanism allowed probes to travel in both the axial and the radial directions. The axial distance of the probe tip from the upstream end of the porous tube was indicated by a Cenco optical bench. The radial position of the probe relative to the tube wall was indicated by a vernier slider reading to the nearest 0.005 cm. Closing of an electric circuit, indicated by lighting-up of a torch bulb, was used to signal the contact of the probe with the tube wall.

5. Test Procedure and Measurements.

a. Velocity Measurements With and Without Wall-Mass Injection. The main air flow was measured by a pitot-static tube placed centrally at x/D = 25 from the leading edge of the entrance tube. The pressure drop and the static pressure were measured with an NIL precision manometer reading to 0.001 in. of water. The temperature at the exit was measured by a thermometer reading to 0.2° F. From these data, centerline velocity of the main air flow was obtained. The axial velocity u, was measured by a hot film anemometer at 10 essentially equal intervals of $(r/R)^2$ at (x/D) = 0, 5, 10, and 20 from the leading edge of the porous tube.

The above test runs were made at main flow Re = 1.5×10^4. Runs were made first without mass injection at the porous tube and then, with uniform air injection along the porous tube at $\overline{m}$ ($= \rho v_w/\rho \bar{u}_o$) = -0.0004.

b. Concentration Measurements with Helium Injection. The concentration of helium distribution was measured with a gas analyzer. Tests were conducted with a fully developed turbulent flow of air in the entrance tube entering the porous tube at Re = 1.5×10^4 and 3×10^4 with uniform helium injection along the porous tube at $\overline{m}$ ($\equiv \dot{m}''_{He}/\rho \bar{u}_o$) = -0.0001, -0.0002, and -0.0004.

For each run, helium concentration, ρ_{He}/ρ, was measured at x/D (from leading edge of the porous tube) = 5, 10, and 20 and at about 15 different r/R positions.

6. Test Results.

a. Velocity Profiles. The measured velocity profiles for the case of no mass injection at the porous tube are plotted in Fig. 8 in the form of $u/\bar{u}_o$ versus $\eta(\equiv r/R)$. The measured velocity profile with air injection at the porous tube is also plotted in Fig. 8 in the form of $u/\bar{u}$ versus η.

b. Helium Concentration Profiles. The measured helium concentrations, f ($\equiv \rho_{He}/\rho$), are plotted versus dimensionless radius, η, in Figs. 9, 10, and 11 for different values of Re (from 1.5×10^4 to 3×10^4), x/D (from 0 to 20), and $\overline{m}$ (from -0.0001 to -0.0004).

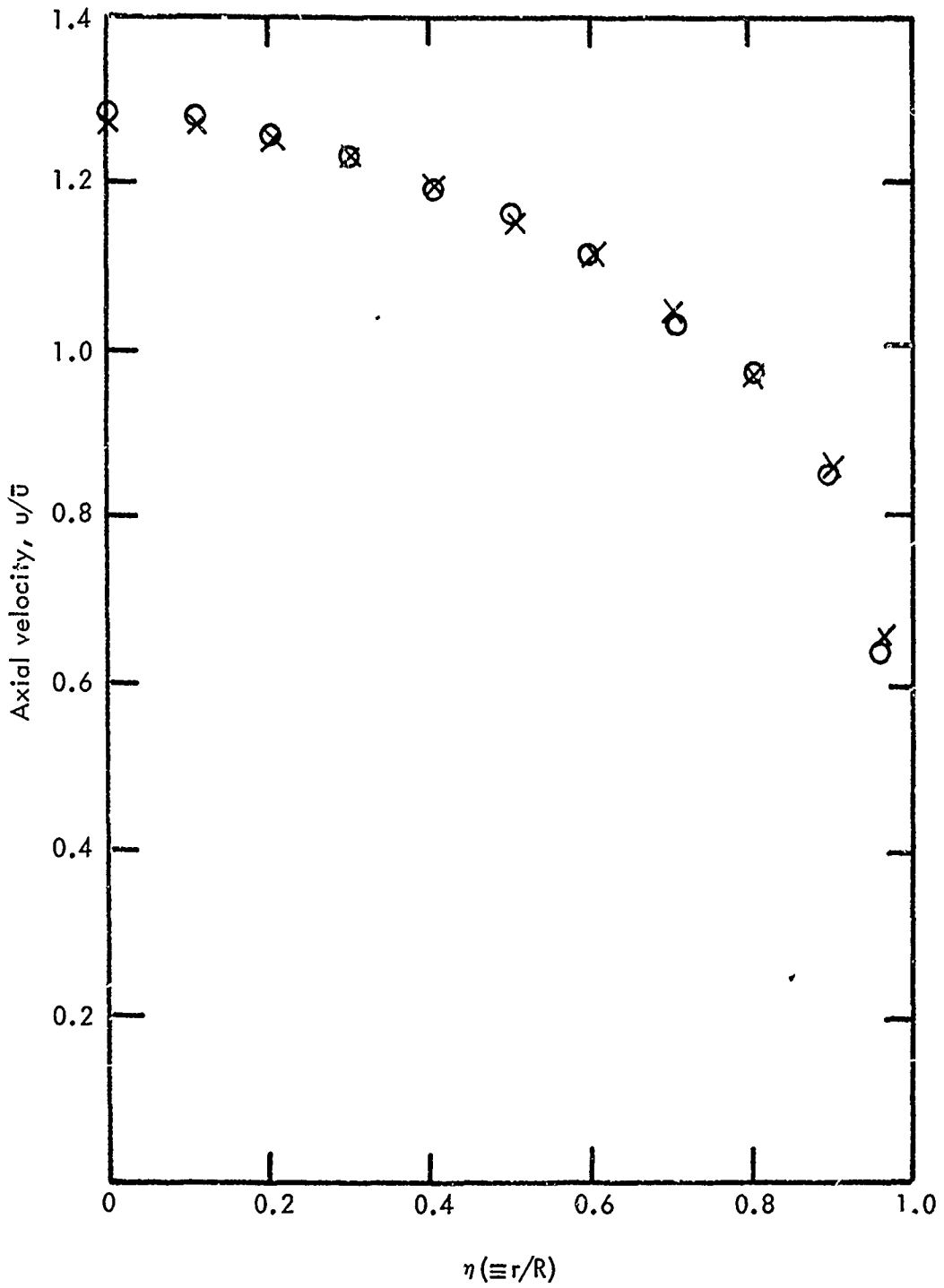

Fig. 8. Measured turbulent velocity profiles at Re = 1.5 x 10^4: X, $\overline{m} = 0$; O, $\overline{m} = -0.0004$.

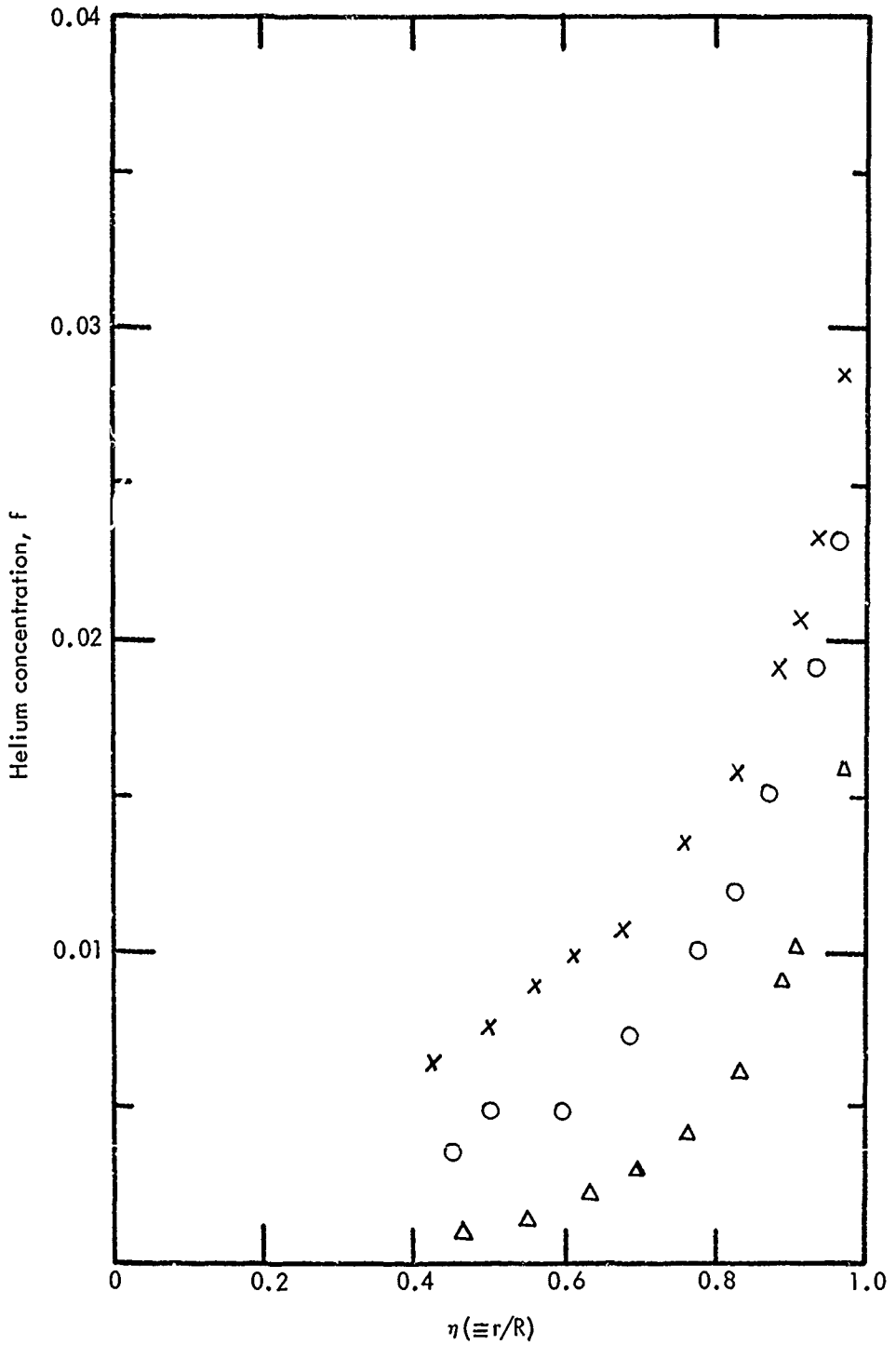

Fig. 9. Measured helium concentration at Re = 1.5 x 10^4 and $\overline{m}$ = -0.0002: X, x/D = 15; O, x/D = 10; Δ, x/D = 5.

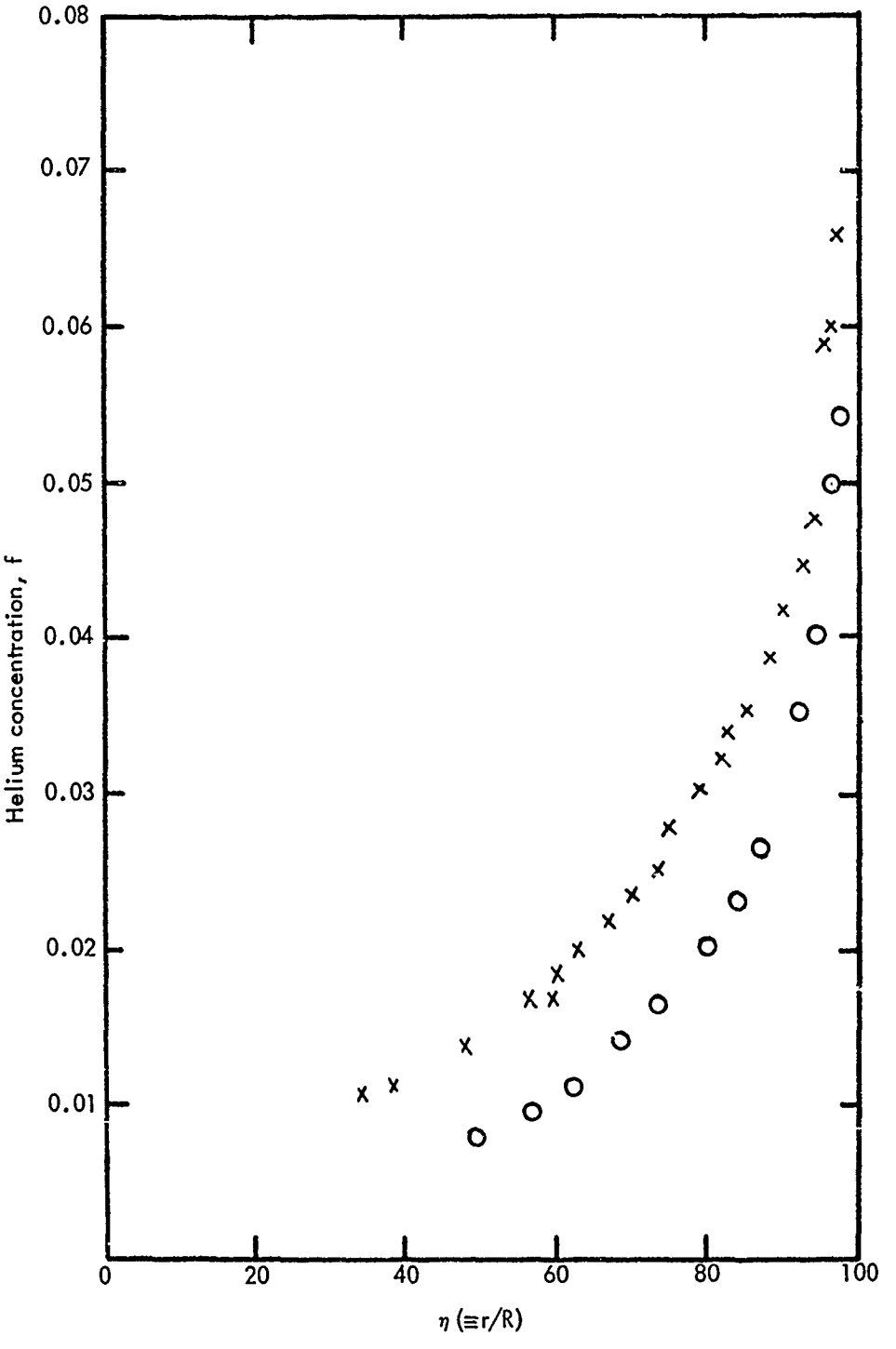

Fig. 10. Measured helium concentration at Re = 1.5 x 10^4 and $\overline{m}$ = -0.0004: X, x/D = 15; O, x/D = 10.

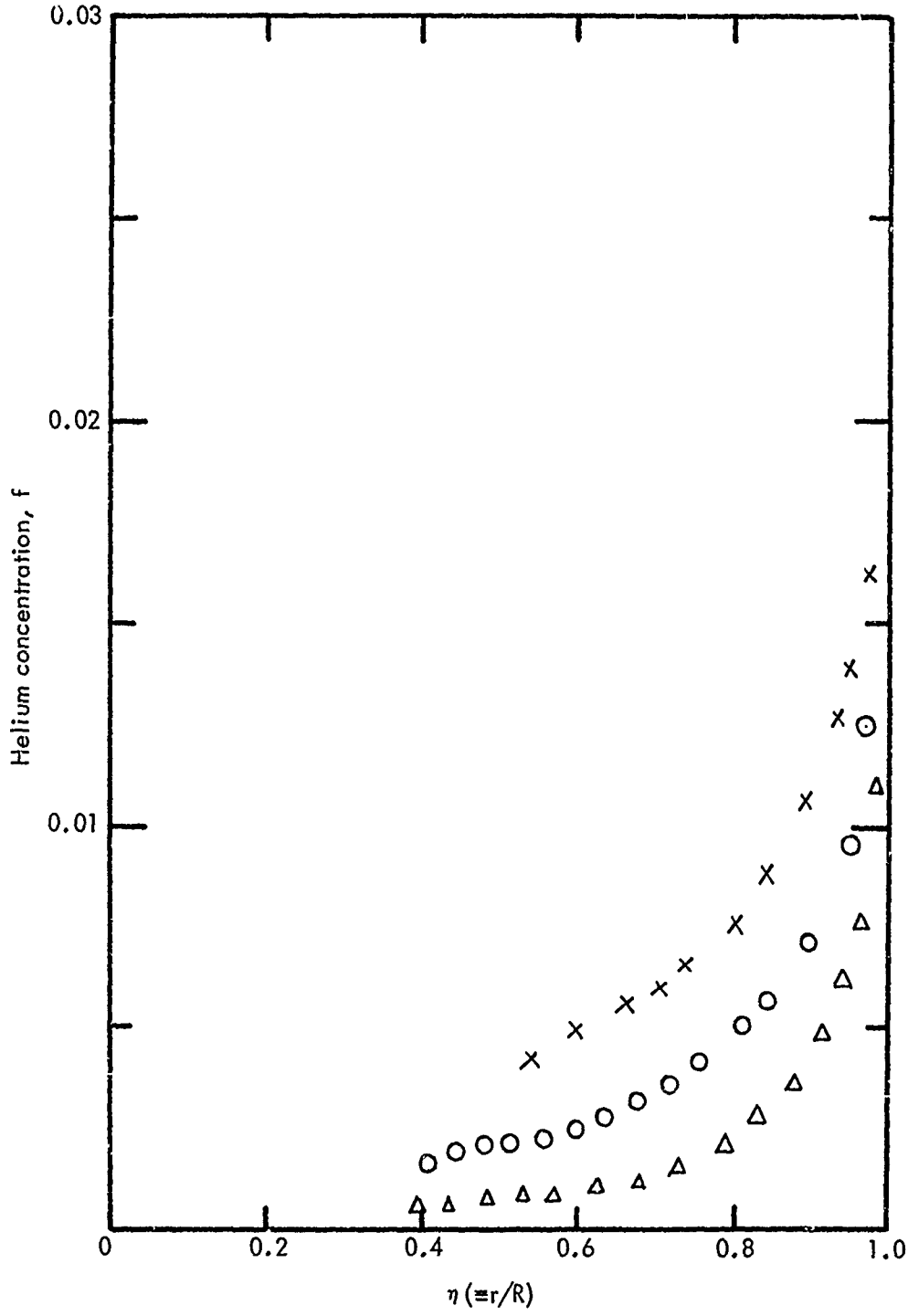

Fig. 11. Measured helium concentration at Re = 3 x 10^4 and $\bar{m}$ = -0.0001: X, x/D = 15; O, x/D = 10; Δ, x/D = 5.

III. THEORETICAL DEVELOPMENT

7. Theoretical Model.

a. **Diffusion Equation.** The problem analyzed is the diffusion of the injected gas, helium for the present investigation, in the fully developed turbulent air flowing in a circular tube as represented by Fig. 12. The conservation equation for the injected helium can be written:

$$\rho u\, \partial f/\partial x + \rho v\, \partial f/\partial r = (1/r)\, \partial(r\rho D_e\, \partial f/\partial r) / \partial r \,. \qquad (1)$$

This equation considers convection in the axial direction and diffusion and convection in the radial direction but neglects axial diffusion. The normalized concentration, f, is the local helium density divided by the mixture density. The latter, following the usual assumption of incompressibility, is considered constant. The boundary conditions to be imposed upon the solution of Equation (1) are

$$\text{At } x=0, \text{ any } r: \quad f=0 \qquad (2)$$

$$\text{At } r=0, \text{ any } x: \quad \partial f/\partial r=0 \qquad (3)$$

$$\text{At } r=R, \text{ any } x: \quad \partial f/\partial r=(1-f)\dot{m}''_w/\rho D \qquad (4)$$

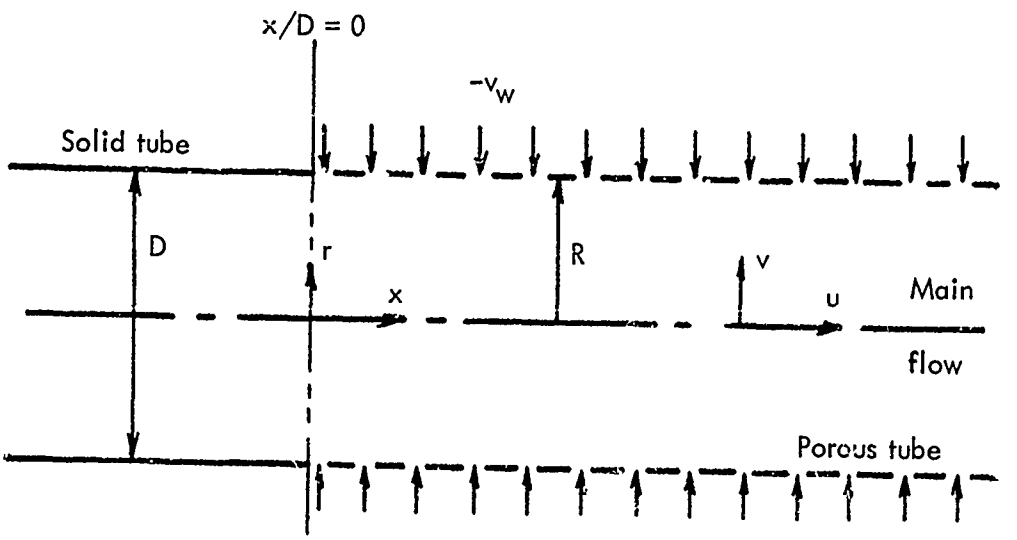

Fig. 12. Nomenclature for flow through a porous tube with injection.

Equation (2) represents the condition that the helium concentration is uniformly zero at the entrance to the leading end of the porous tube; Equation (3) implies axisymmetry with respect to the tube centerline; and Equation (4) relates helium diffusion and convection at the porous tube surface to helium injection rate per unit area, $\dot{m}_w''$. It is also implied in Equation (4) that turbulence is completely damped at the tube surface; thus, the effective diffusivity, D_e, at r=R is replaced by the molecular diffusivity of helium in air, D.

To integrate Equation (1) with boundary conditions, Equations (2) through (4), the turbulent velocity field, u and v, and the effective diffusivity, D_e, must first be specified. Consideration is given below to the mathematical representation of these quantities.

b. Turbulent Velocity Field. A complete solution for the velocity field requires numerical integration of continuity and momentum equations. However, when the nondimensional mass injection rate, $\bar{m}(\equiv \dot{m}_w''/\rho\bar{u})$, is small, it can be expected that the fully developed turbulent velocity profile at the entrance to the porous tube will not be distorted. It seems reasonable for the present investigation at $\bar{m} = -0.0001$ to -0.0004 to assume that the axial velocity profile can be represented by

$$u = \bar{u}\,\phi_o(\eta) \tag{5}$$

where $\phi_o(\eta)$ is the fully developed turbulent velocity profile, $u/\bar{u}$, at entrance to the porous tube, i.e. at x=0, and $\bar{u}$ at the other axial position can be calculated by the equation

$$\bar{u}=\bar{u}_o\,(1+2\bar{m}\xi)\,. \tag{6}$$

Substitution of Equations (5) and (6) in the continuity equation

$$\partial ur/\partial x+\partial vr/\partial r = 0 \tag{7}$$

followed by integration yields the following expression for the radial velocity distribution

$$v = (-2\bar{m}\bar{u}/\eta)\int_0^{\eta} \phi_o\,\eta d\eta\,. \tag{8}$$

Hence u and v distribution for specified $\bar{u}_o$ and $\bar{m}$ can be evaluated if $\phi_o(\eta)$ is determined.

It is shown in Appendix A that $\phi_o(\eta)$ can be evaluated by the equation

$$\phi_o(\eta) = \left\{ \int_\eta^1 2R^+\eta \left\{1+\left\{1+4\eta(R^+)^2 \left\{(0.14-0.08\eta^2-0.06\eta^4)(1-\exp(-R^+ (1-\eta)/A))\right\}^2\right\}^{1/2}\right\}^{-1} d\eta \right\} \div \left\{ 2\int_0^1 \eta \int_\eta^1 2R^+\eta \left\{1+\left\{1+4\eta(R^+)^2 \left\{(0.14 -0.08\eta^2-0.06\eta^4)(1-\exp(-R^+(1-\eta)/A))\right\}^2\right\}^{1/2}\right\}^{-1} d\eta\, d\eta \right\} \quad (9)$$

where R^+ is related to the entrance Reynolds number, Re. This relation is shown graphically by Fig. 13. Figure 14 shows the calculated $\phi_o(\eta)$ at Re = 2×10^3 to 1×10^6.

c. **Effective Diffusivity for Turbulent Flow.** The effective diffusivity, D_e, can be obtained by use of a formula[12] of the form

$$D_e = \mu/\rho Sc + \mu_t/\rho Sc_t \quad (10)$$

where ρ is the density of the air, μ is the laminar viscosity of the air, Sc is the laminar Schmidt number of helium in air, Sc_t is the turbulent Schmidt number which is a constant of 0·86, and μ_t is the turbulent viscosity. Among the various candidate representations for the turbulent viscosity, a model involving Prandtl's mixing length and Van Driest's damping factor has gained broad acceptance in recent years.[13-18]

This approach is employed here and gives the following model for the turbulent viscosity:

---

[12] S. V. Patankar and D. B. Spalding, "Heat and Mass Transfer in Boundary Layers," Morgan and Grampin, London (1967).

[13] R. B. Kinney and E. M. Sparrow, "Turbulent Flow Heat Transfer, and Mass Transfer in a Tube with Surface Suction," ASME Paper No. 69-HT-4 (1969).

[14] E. M. Sparrow, V. K. Jonsson, G. S. Beavers, and R. G. Over, "Incompressible Turbulent Flow in a Permeable Wall Duct," ASME Paper No. 71-WA/FE-1 (1971).

[15] T. Cebeci, A. M. O. Smith, and G. Mosinskis, "Solution of the Incompressible Turbulent Boundary-Layer Equations," *J. Heat Transfer*, Vol. 92, pp. 133-143 (1970).

[16] S. V. Patankar and D. B. Spalding, "Heat Transfer in Boundary Layers," Morgan and Grampin, London (1967).

[17] S. W. Chi and C. C. Chang, "Effective Viscosity in a Turbulent Boundary Layer," *AIAA Journal*, Vol. 7, pp. 2032-2035 (1969).

[18] W. J. Glowacki and S. W. Chi, "Effect of Pressure Gradient on Mixing Length for Equilibrium Turbulent Boundary Layers," AIAA Paper No. 72-213 (1972).

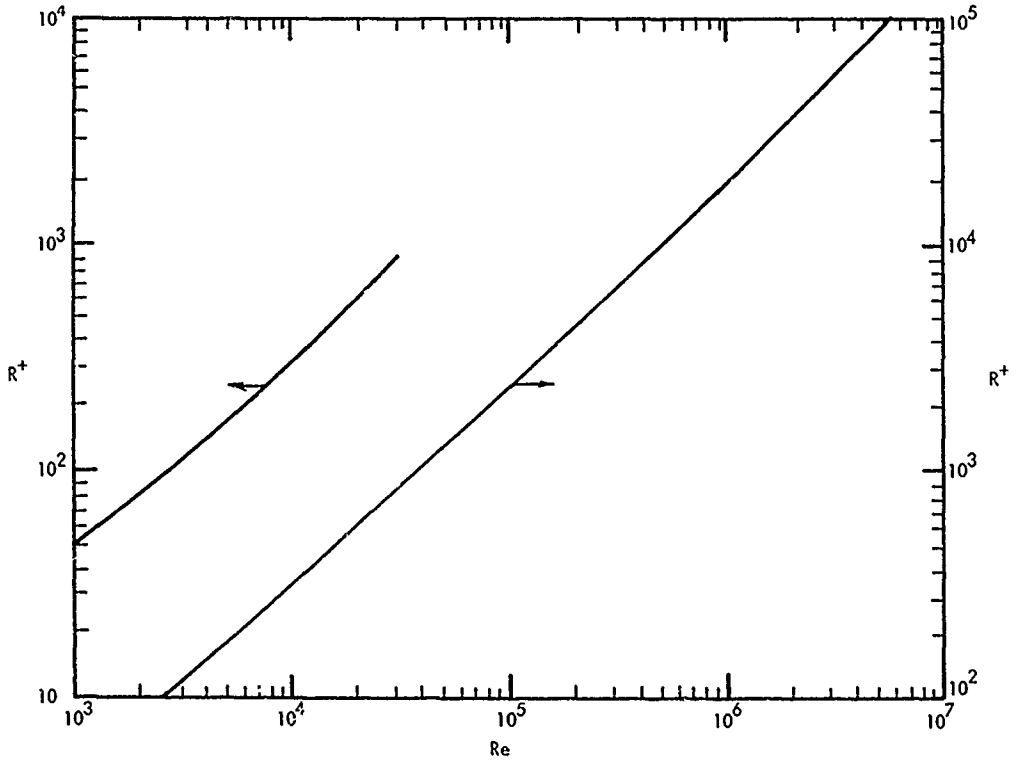

Fig. 13. Reynolds number, Re, versus nondimensional tube radius, R^+.

$$\mu_t = \rho l^2 |\partial u/\partial r| \tag{11}$$

$$1/R = DF\,(0.14-0.08\eta^2-0.06\eta^4) \tag{12}$$

$$DF = 1-\exp\left\{-\chi-1/\sqrt{2}\,[\,(\chi^4+4\,(R^+(1-\eta)/A)^4\,]^{1/2}+\chi^2\,\right\}^{1/2} \tag{13}$$

where χ is defined as $\overline{m}Re\,(1-\eta)/4$. Equation (11) expresses Prandtl's mixing length concept, while Equation (12) is a representation for the mixing length, l, deduced by Nikuradse[19] from measured velocity profiles for the circular tube. Van Driest's damping factor[20] generalized by Kinney and Sparrow[21] is expressed by Equation (13).

[19] H. Schlichting, "Boundary Layer Theory," McGraw-Hill, New York (1968).

[20] E. R. Van Driest, "On Turbulent Flow Near a Wall," *J. Aero. Sci.*, Vol. 23, pp. 1006-1011, 1036 (1956).

[21] R. B. Kinney and E. M. Sparrow, "Turbulent Flow, Heat Transfer, and Mass Transfer in a Tube with Surface Suction," ASME Paper No. 69-HT-4 (1969).

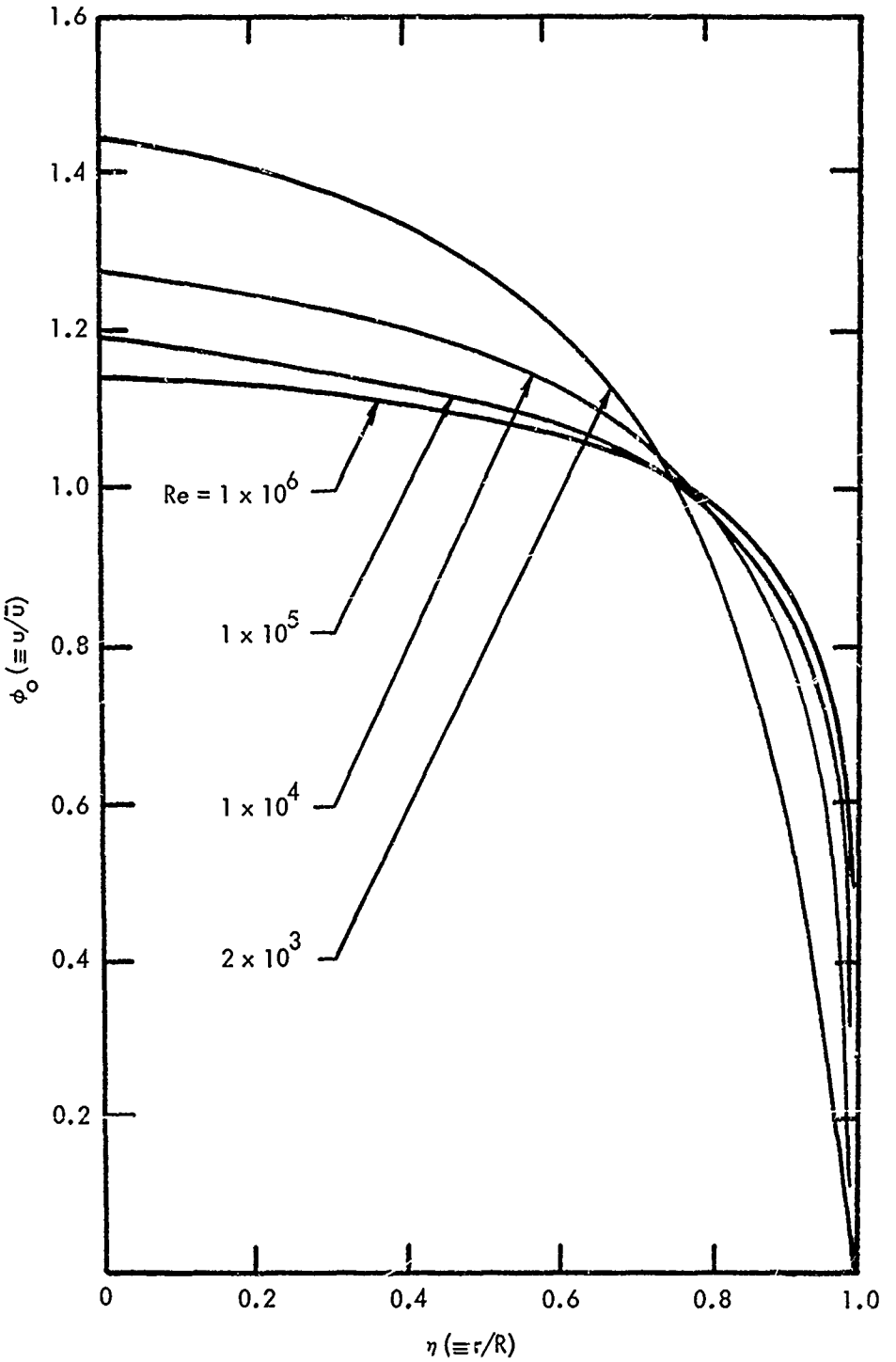

Fig. 14. Calculated velocity profile at Re = 2 x 10^3 to 1 x 10^6.

Combining Equations (10) through (13), followed by rearrangement, yields a $\bar{D}_e$ ($\equiv D_e/\nu$) expression:

$$\bar{D}_e = 1/Sc + [0.5\,Re\,(1+2\bar{m}\xi)/Sc_t] \left\{ [1-\exp\left\{-\chi-1/\sqrt{2}\,[\,(\chi^4+4\,(R^+\,(1-\eta)/26)^4\,]^{1/2}+\chi^2\right\}^{1/2}] \,(0.14-0.08\eta^2-0.06\eta^4)\right\}^2 \cdot |d\phi_o/d\eta| \qquad (14)$$

d. **Nondimensional Diffusion Equation.** The diffusion Equation (1) and its boundary conditions represented by Equations (2) through (4) can now be transformed into the following nondimensional form:

$$U(\partial f/\partial\xi) + V(\partial f/\partial\eta) = (1/\eta)\,\partial\,(\eta\bar{D}_e\partial f/\partial\eta)/\partial\eta \qquad (15)$$

$$\text{At } \xi=0, \text{ any } \eta\text{: } f=0 \qquad (16)$$

$$\text{At } \eta=0, \text{ any } \xi\text{: } \partial f/\partial\eta=0 \qquad (17)$$

$$\text{At } \eta=1, \text{ any } \xi\text{: } \partial f/\partial\eta=0.5\,Re\bar{m}\,Sc(1-f) \qquad (18)$$

$$\text{where } U=0.5Re\,(1+2\bar{m}\xi)\,\phi_o \qquad (19)$$

$$V=(-Re\,\bar{m}/\eta)\int_0^\eta \eta\phi_o\,d\eta \qquad (20)$$

and $\overline{D_e}$ and ϕ_o are evaluated by Equations (9) and (14) respectively.

8. **Solution of Diffusion Equation by Finite Difference.**

a. **Finite Difference Scheme.** A two-layer implicit finite difference procedure given by Crank and Nicholson[22] is developed to solve the dimensionless diffusion Equation (15) with boundary conditions of Equations (16) to (18). Values of U, V, and $\overline{D_e}$ from known values of Sc and m are first calculated by Equations (19), (20), and (14) respectively. Using a rectangular grid system in (ξ, η) plane with

$$\xi_{i+1} = \xi_i + \Delta\xi_i \qquad (21)$$

$$\eta_{j+1} = \eta_j + \Delta\eta_j\,, \qquad (22)$$

[22] J. Crank and P. Nicholson, "A Practical Method for Numerical Evaluation of Solutions of Partial Differential Equations of Heat Conduction Type," *Proc. Cambridge Phil. Soc.*, Vol. 43, p. 50 (1967).

partial differential Equation (15) is approximated at the midpoint $(\xi_{i+\frac{1}{2}}, \eta_j)$ as follows:

$$\alpha_j f_{j-1}^{i+1} + \beta_j f_j^{i+1} + \gamma_j f_{j+1}^{i+1} = \delta_j \tag{23}$$

where

$$\alpha_j = -(\eta \bar{D}_e)_{j-\frac{1}{2}}^{i+\frac{1}{2}} / 2\eta_j (\Delta\eta_j)^2 - V_j^{i+\frac{1}{2}} / 4(\Delta\eta_j) \tag{24}$$

$$\beta_j = U_j^{i+\frac{1}{2}} / \Delta\xi_i + [(\eta \bar{D}_e)_{j+\frac{1}{2}}^{i+\frac{1}{2}} + (\eta \bar{D}_e)_{j-\frac{1}{2}}^{i+\frac{1}{2}}] / 2\eta_j (\Delta\eta_j)^2 \tag{25}$$

$$\gamma_j = V_j^{i+\frac{1}{2}} / 4(\Delta\eta_j) - (\eta \bar{D}_e)_{j+\frac{1}{2}}^{i+\frac{1}{2}} / 2\eta(\Delta\eta_j)^2 . \tag{26}$$

$$\delta_j = f_{j-1}^{i} [(\eta \bar{D}_e)_{j-\frac{1}{2}}^{i+\frac{1}{2}} / 2\eta_j (\Delta\eta_j)^2 + V_j^{i+\frac{1}{2}} / 4(\Delta\eta_j)]$$

$$+ f_j^{i} \left\{ U_j^{i+\frac{1}{2}} / \Delta\xi_i - [(\eta \bar{D}_e)_{j+\frac{1}{2}}^{i+\frac{1}{2}} + (\eta \bar{D}_e)_{j-\frac{1}{2}}^{i+\frac{1}{2}}] / 2\eta_j (\Delta\eta_j) \right\}^2$$

$$+ f_{j+1}^{i} [(\eta \bar{D}_e)_{j+\frac{1}{2}}^{i+\frac{1}{2}} - V_j^{i+\frac{1}{2}} / 4(\Delta\eta_j)] . \tag{27}$$

The grid point spacings are written as $\Delta\xi_i$ and $\Delta\eta_j$ to indicate that they can be varied in the different parts of the grid. Coefficients, α_j, β_j, γ_j, and δ_j written above are valid for $\Delta\eta_{j-1} = \Delta\eta_j$. In the present application, however, it was found best to use a small interval near the wall and to halve the interval a number of times as η increased as shown in the Table.

Variation of $\Delta\eta$

j	η	$\Delta\eta$
0- 39	0 to 0.512	0.0128
40- 79	0.512 to 0.768	0.0064
80-119	0.768 to 0.896	0.0032
120-159	0.896 to 0.960	0.0016
160-199	0.960 to 0.992	0.0008
200-209	0.992 to 0.996	0.0004
210-219	0.996 to 0.998	0.0002
220-240	0.998 to 1.000	0.0001

If the interval is halved at successive values of j, i.e., $\Delta\eta_{j-1} = 2\,\Delta\eta_j = \Delta\eta_j + \Delta\eta_{j+1}$, the appropriate expressions for the coefficients α_j, β_j, γ_j, and δ_j are obtained from Equations (24) through (27) by replacing j+1 with j+2.

The computing procedure involves calculation of the concentration profiles. At successive increments of ξ, employing Equation (23) to extrapolate to the new concentration $f(\xi_i+\Delta\xi_i, \eta)$ from previous $f(\xi_i, \eta)$ using forcing coefficients:

$$A_j = -\gamma_j/(\alpha_j A_{j-1} + \beta_j) \tag{28}$$

$$B_j = (\delta_j-\alpha_j B_{j-1}) / (\alpha_i A_{j-1} + \beta_j) \tag{29}$$

for $\Delta\eta_j = \Delta\eta_{j-1}$, and

$$A_j = \gamma_j\beta_{j+1} / [\gamma_{j+1} (\alpha_j A_{j-1} + \beta_j) - \gamma_j\alpha_{j+1}] \tag{30}$$

$$B_j = [\gamma_{j+1} (\delta_j-\alpha_j\beta_{j-1}) - \gamma_j\delta_{j+1}]/[\gamma_{j+1} (\alpha_j A_{j-1}+\beta_j) - \gamma_j\alpha_{j+1}] \tag{31}$$

for $\Delta\eta_j = 1/2\Delta\eta_{j-1}$. The values of f_j^{i+1} are calculated from the recursion formula

$$f_j^{i+1} = A_j f_{j+1}^{i+1} + B_j \tag{32}$$

provided A_o, B_o at the centerline and f_n^{i+1} at the tube wall are both known.

b. Coefficients at Centerline, A_o and B_o. At the centerline, $V = \partial\phi_o/\partial\eta=0$ because of symmetry; diffusion Equation (15) is reduced to the form

$$U\partial f/\partial\xi = (1/\eta Sc) [\eta\partial^2 f/\partial\eta^2 + \partial f/\partial\eta]. \tag{33}$$

Equation (33) is indeterminate at the centerline, as is its corresponding finite difference form, because of the indeterminate terms $(1/\eta)\,\partial f/\partial\eta$. In the limit, as $\eta\to 0$, using L'Hospital rule, this indeterminate term may be replaced by its corresponding determinate form. The centerline differential Equation (33) thus has the form

$$U\partial f/\partial\xi = (2/Sc) (\partial^2 f/\partial\eta^2). \tag{34}$$

Noting the boundary condition, Equation (17),

$$\text{At } \eta=0:\ \partial f/\partial\eta=0 \quad \text{i.e., } f_{-1}^{i+1}=f_{+1}^{i+1}. \tag{35}$$

Equation (34) can be written in the following finite difference form:

$$f_0^{i+1} = A_0 f_1^{i+1} + B_0 \tag{35A}$$

where $A_0 = 2/ [Sc(\Delta\eta)^2 (U_0^{i+1/2} / \Delta\xi + 2/Sc(\Delta\eta)^2]$ (36)

and $B_0 = [U_0^{i+1/2} / \Delta\xi - 2/Sc(\Delta\eta)^2] f_0^i + 2f_1^i / Sc(\Delta\eta)^2 /$

$$[U_0^{i+1/2} / \Delta\xi + 2/Sc(\Delta\eta)^2] . \tag{37}$$

With A_o and B_o calculated by Equations (36) and (37) respectively, A_j and B_j with $j = 1, 2, \text{---} (n-2)$ can be evaluated with Equations (28) and (29) or (30) and (31), whichever is appropriate.

c. **Wall Concentration, f_n^{i+1}.** For evaluation of wall concentration f_n^{i+1}, we begin with the boundary condition, Equation (18):

At $\eta=1$: $\partial f/\partial\eta = ReScm(1-f)$.

Its corresponding finite difference form can be written as

$$f_n^{i+1} = f_{n-1}^{i+1} - \Delta\eta ReSc\bar{m} (1 - f_{n-1}^{i+1}) . \tag{38}$$

Substituting Equation (38) into Equation (23) with $j = n-1$ yields

$$\alpha'_{n-1} f_{n-2}^{i+1} + \beta'_{n-1} f_{n-1} = \delta_n \tag{39}$$

where $\alpha'_{n-1} = \alpha_{n-1}$ (40)

$$\beta'_{n-1} = \beta_{n-1} + (1+\Delta\eta ReSc\, \bar{m})\, \gamma_{n-1} \tag{41}$$

$$\delta'_{n-1} = \delta_{n-1} + \gamma_{n-1}\, \Delta\eta ReSc\bar{m} . \tag{42}$$

Elimination of f_{n-2}^{i+1} between Equations (39) and (32) with $j = n-2$ yields the following solution for f_{n-1}^{i+1}:

$$f_{n-1}^{i+1} = (\delta'_{n-1} - \alpha'_{n-1}\, B_{n-2}) / (\alpha'_{n-1}\, A_{n-2} + \beta'_{n-1}) . \tag{43}$$

Then f_n^{i+1} can be calculated by Equation (37); i.e.,

$$f_n^{i+1} = (1+\Delta\eta ReScm)\, f_{n-1}^{i} - \Delta\eta ReScm, \qquad (44)$$

and f_{n-1}^{i+1} to f_0^{i+1} can be calculated by the recursion Equation (32).

Thus, the problem is represented by Equation (43) for j=n-1, Equation (44) for j=n, and Equation (32) for j=n-2, n-3, ---0, together with initial condition, Equation (16).

d. Sequence of Computations and Computer Program. The procedure for solution of the diffusion problem can now be outlined by the following sequence of operations:

(1) Input parameters, Reynolds number Re, Schmidt number Sc, and mass injection rate $\overline{m}$ are set.

(2) R^+ value corresponding to given Re is read from Fig. 13.

(3) The entrance velocity profile $\phi(\eta)$ is calculated from Equation (9):

(4) U, V, and $\overline{D}_e$ are calculated by Equations (19), (20), and (14), respectively.

(5) $\alpha_j, \beta_j, \gamma_j$, and δ_j are evaluated by Equations (24), (25), (26), and (27) respectively.

(6) A_o and B_o are calculated by Equations (36) and (37), respectively.

(7) A_j and B_j with j = 1, 2, -- (n-2), are evaluated by Equations (28) and (29) for $\Delta\eta_j=\Delta\eta_{j-1}$ or by Equations (30) and (31) for $\Delta\eta_j=1/2\Delta\eta_{j-1}$.

(8) f_{n-1}^{i+1} and f_n^{i+1} are evaluated by Equations (43) and (44).

(9) f_j^{i+1}, with j = (n-2), (n-3), --0, is evaluated by Equation (32).

(10) The value of i is incremented by unity, and steps (4) through (9) are repeated until the concentration field is computed for the desired value of ξ.

A computer program in Fortran IV Language has been written and is appended for the above sequence of operations. In this program, $\Delta\eta_j$'s are specified in accordance with the Table, and the initial $\Delta\xi$ was chosen to be 10^{-6}. Then, the successive $\Delta\xi$ was twice of the previous $\Delta\xi$, or 0.5, whichever was smaller.

For the convenience of the users of the present theory, the complete program listing, together with users' instruction, may be found in Appendix B. Examples of calculated helium concentration field at Re = 1 x 10^4 to 1 x 10^6 and $\bar{m}$ = -0.001 are plotted in Figs. 15 through 17.

IV. RESULTS AND DISCUSSION

9. Summary of Results. Experimental and theoretical investigations of turbulent diffusion in round tubes have been made.

Experiments were carried out with fully developed turbulent flows of air at Re = 15,000 and 30,000 entering a porous tube with circular cross section. Measurements of velocity distribution were made when air was injected uniformly through the tube wall for 36 radii at various ratios of mass velocity through the tube wall to the average mass velocity at the entrance cross section of the tube ranging from 0 and 0.0004. These data are plotted in Fig. 8.

Measurements of helium concentration were also made at Re = 1.5 x 10^4 and 3 x 10^4 when helium was injected uniformly through the tube wall for 36 radii at various ratios of helium mass velocity through the tube wall to the mass velocity of air at the entrance cross section of the tube ranging from 0.0001 to 0.0004. These data are summarized in Figs. 9 through 11.

A finite difference procedure for turbulent diffusion was developed based upon the mixing-length concept for the turbulent diffusivity and the assumption that for small wall injection the distortion of velocity profile, $u/\bar{u}$, due to mass injection is negligible. A computer program in Fortran IV language has been written in accordance with the developed calculation procedure. Examples of calculated helium concentration distribution at Re = 5 x 10^3 to 1 x 10^5 and $\bar{m}$ equal to -0.001 are plotted in Figs. 15 through 17.

However, the significance in a finite difference solution of any physical problem lies in the accuracy of the finite difference scheme and the adequacy of the assumptions made. The remainder of this section is devoted to verifying the accuracy of the present numerical scheme and physical assumptions.

10. Accuracy of Calculation Scheme. Accuracy of the calculation scheme can be measured by comparing the solution with the known exact solution. Since no exact solution is available for turbulent flow, tests for accuracy will first be made by comparing the present data with the more exact solution for laminar flow[23] and with correlated

[23] G. Raithby, "Laminar Heat Transfer in the Thermal Entrance Region of Circular Tubes and Two-Dimensional Rectangular Ducts with Wall Suction and Injection," *Int. J. Heat Mass Transfer*, Vol. 14, pp. 223-243 (1971).

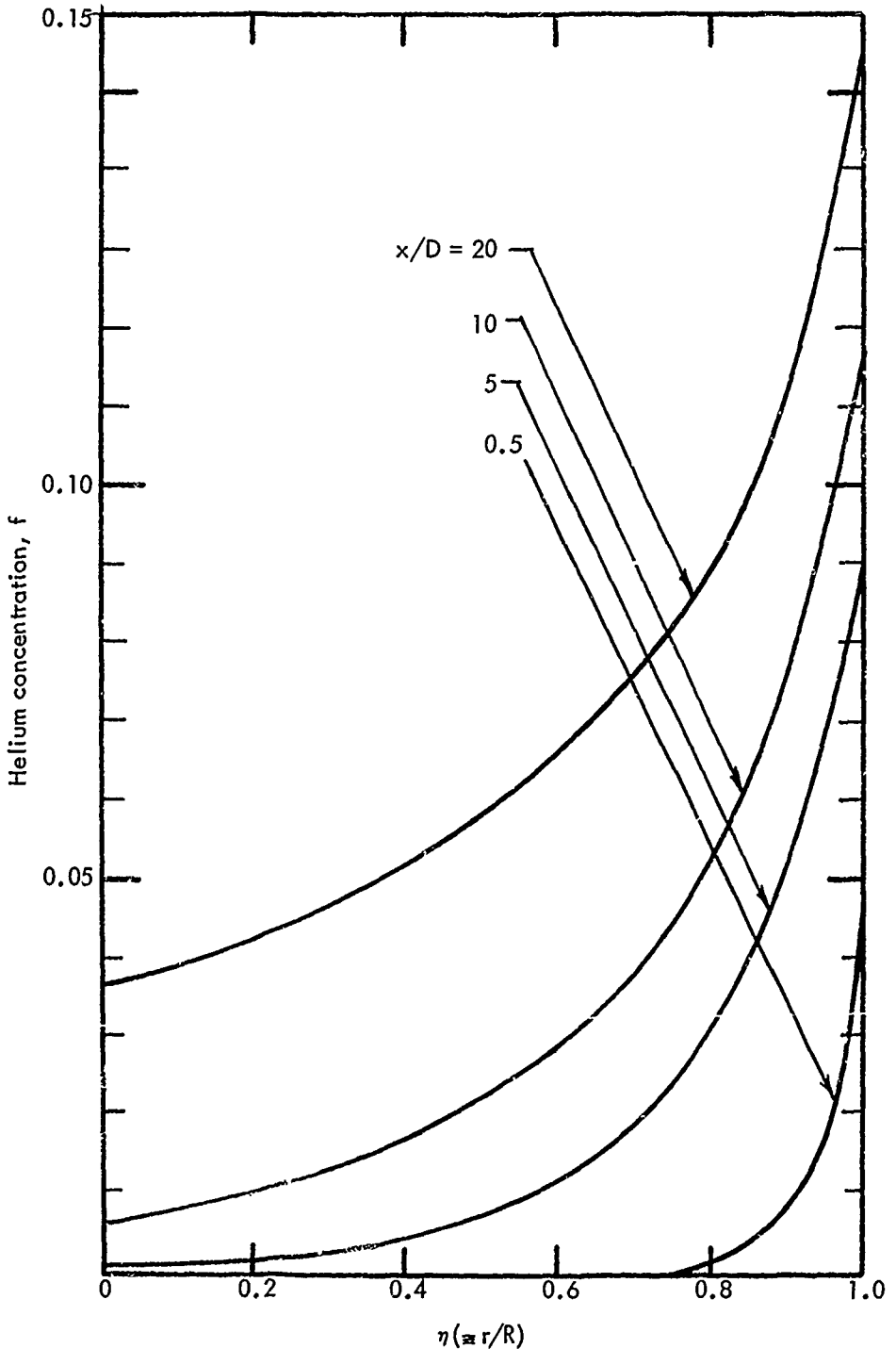

Fig. 15. Calculated helium concentration profiles at Re = 5 x 10^3 and $\overline{m}$ = -0.001.

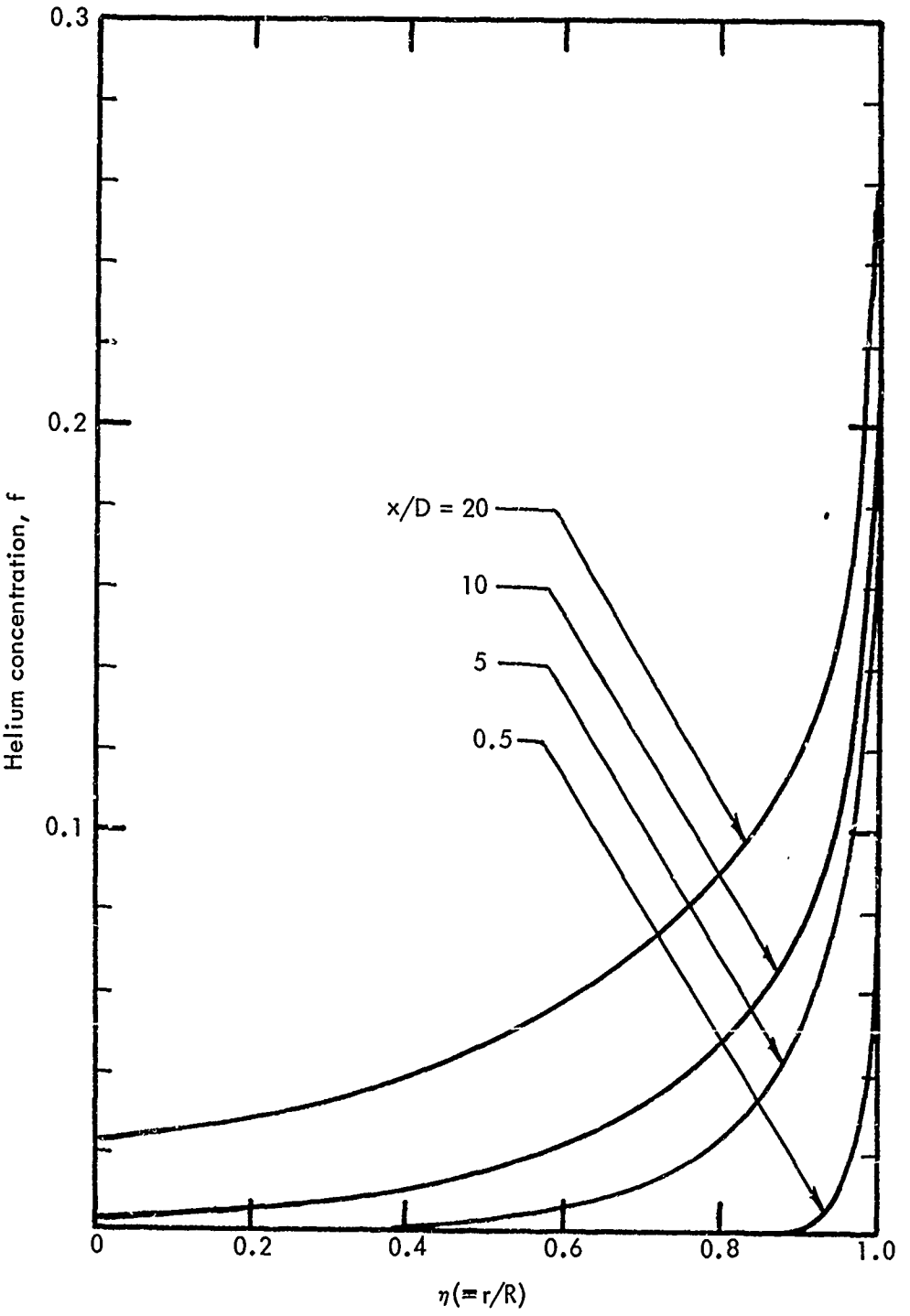

Fig. 16. Calculated helium concentration profiles at Re = 5 x 10^4 and $\overline{m}$ = -0.001.

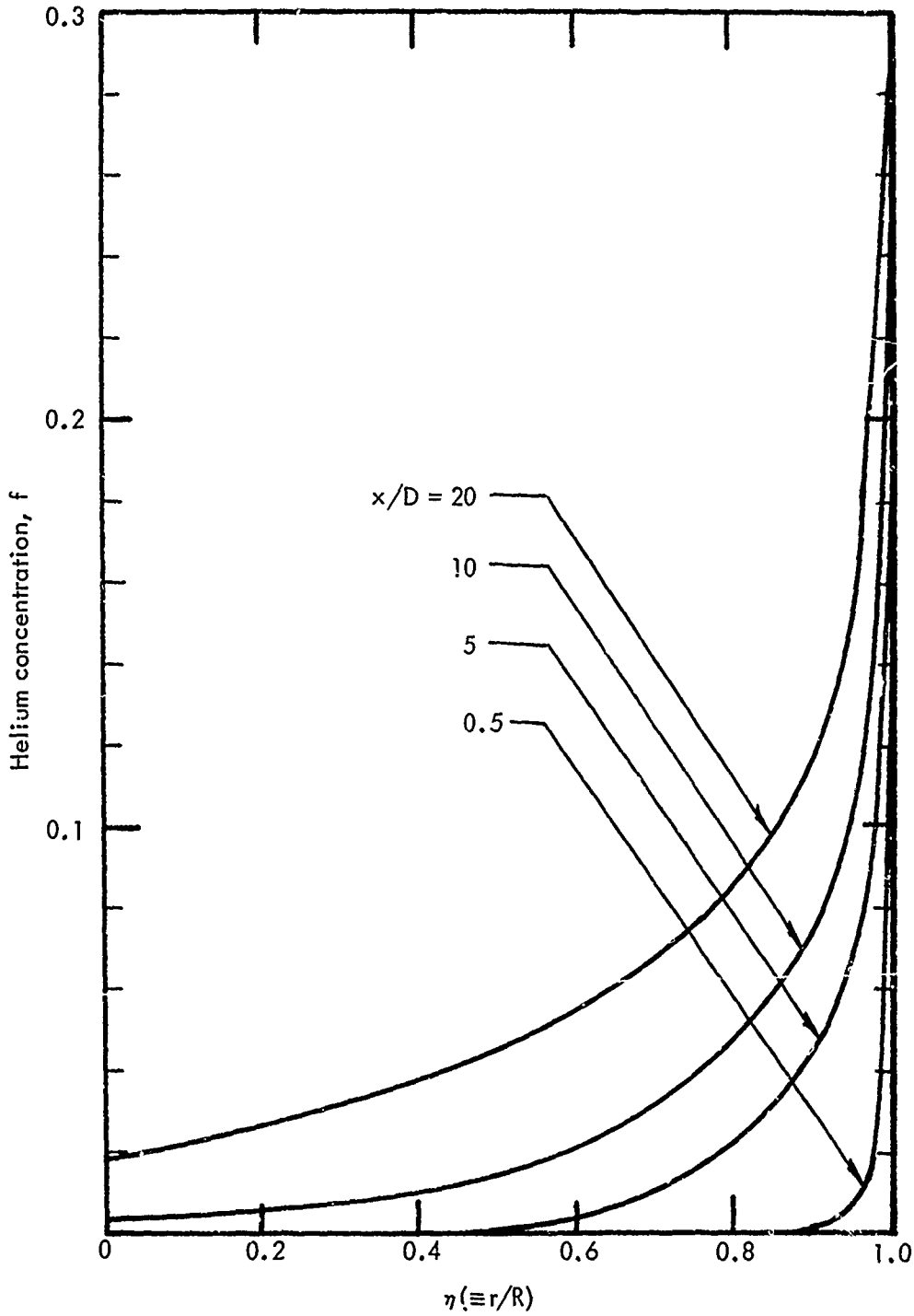

Fig. 17. Calculated helium concentration profiles at Re = 1 x 10^5 and $\overline{m}$ = -0.001.

heat transfer data for zero wall injection.[24]

The exact solution for laminar heat transfer with wall mass injection has been obtained by Raithby[25] . In order to compare his solutions with our numerical solution, the present computer program has been modified by replacing the turbulent velocity profile ϕ_0 (η) with the well-known parabolic velocity profile for laminar flow and replacing the dimensionless effective diffusion, $\overline{D}_e$, with the laminar exchange coefficient, 1/Pr. Figure 18 shows a comparison of the present solution of temperature profiles with Raithby's exact solution under the same conditions. Figure 19 shows a comparison of Nusselt numbers at the thermal entrance region calculated by the present method with those calculated by Raithby.

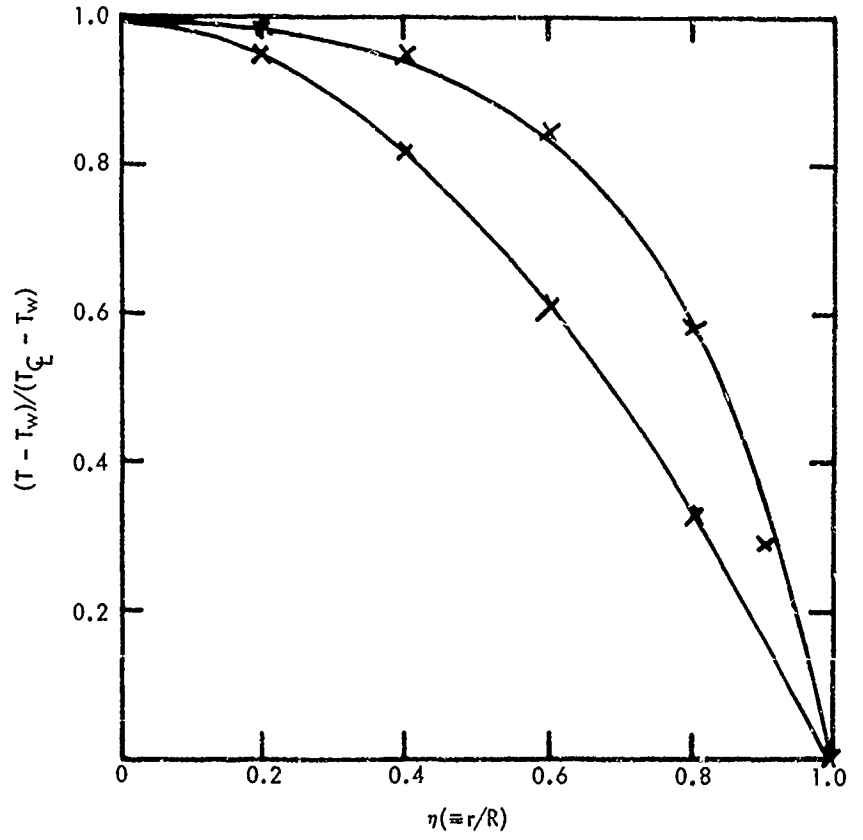

Fig. 18. Comparison of temperature profiles for laminar flow with constant heat flux and uniform wall injection: —, exact solution from Raithby; X, present theory.

[24] W. M. Kays, "Convective Heat and Mass Transfer," McGraw-Hill, New York (1966).

[25] G. Raithby, "Laminar Heat Transfer in the Thermal Entrance Region of Circular Tubes and Two-Dimensional Rectangular Ducts with Wall Suction and Injection," *Int. J. Heat Mass Transfer*, Vol. 14, pp. 223-243 (1971).

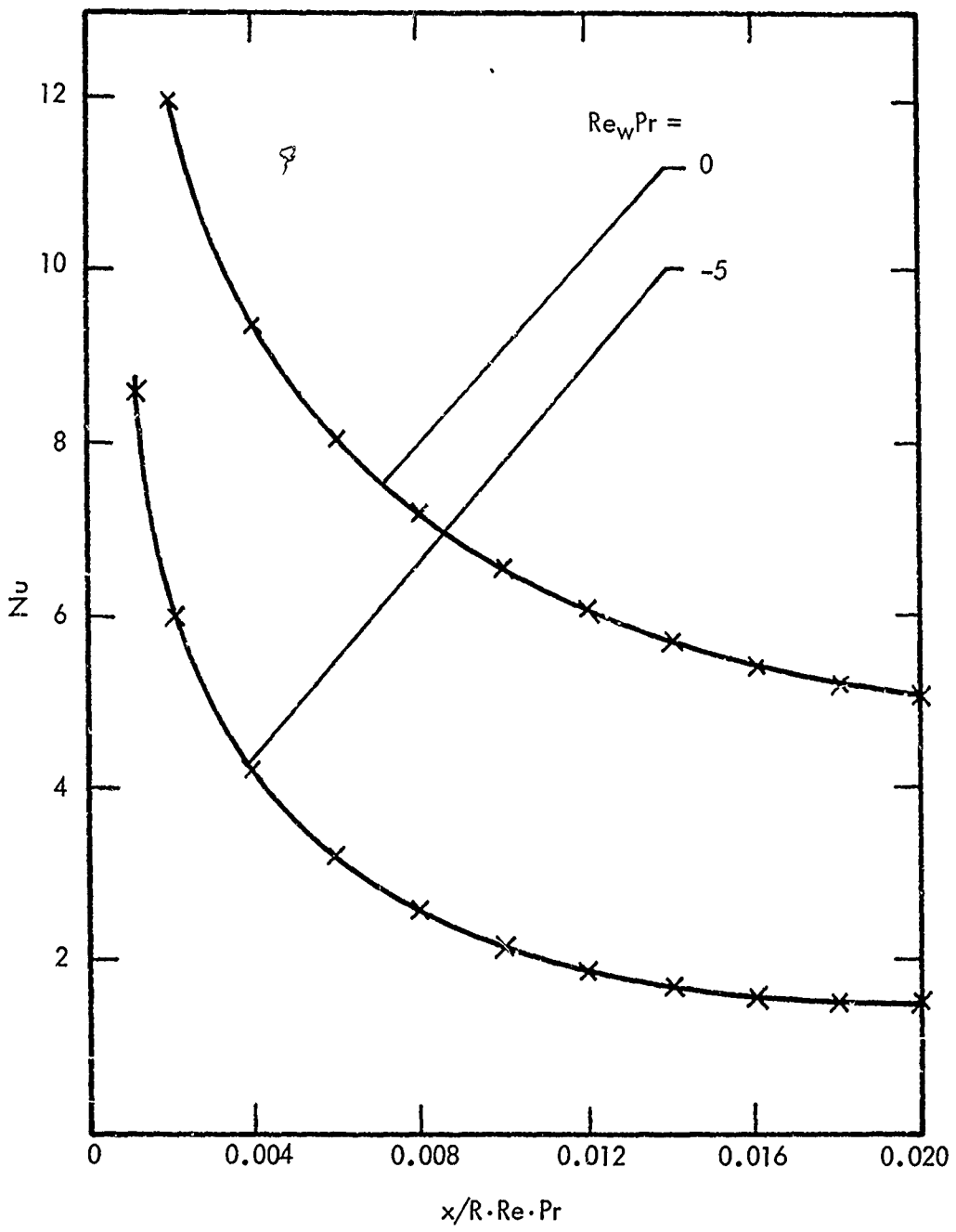

Fig. 19. Comparison of Nusselt number for laminar flow with constant heat flux: —, exact solution from Raithby; X, present theory.

Turbulent heat-transfer data with zero wall-mass transfer has been correlated by Kays.[26] In order to compare the present solution with Kays' correlation, the present program was modified by replacing the Schmidt number, Sc, by the Prandtl number, Pr. Figure 20 shows a comparison of the fully developed Nusselt number, Nu, calculated by the present method with that correlated by Kays. Figure 21 shows a comparison of the Nusselt number for turbulent heat transfer in the thermal entrance region.

It can be seen in Figs. 18 through 21 that the present results are consistently in agreement with the available laminar and turbulent heat transfer data with and without wall-mass transfer.

11. Justification of Main Assumption and Comparison with Experiments. The main assumption made in the present analysis is that the velocity profile, $u/\bar{u}$, is insensible to the wall-mass transfer at the range of wall-mass flux, $\bar{m}$, ranging from 0.0001 to 0.0004. This assumption is justified by examining Fig. 22 where the measured $u/\bar{u}$, derived from the experimental data of Fig. 8 and the theoretical data of Equation (9), is plotted.

Finally, the overall accuracy of the present solutions for the turbulent diffusion in round tube is compared with the experimental data under the same conditions in Figs. 23, 24, and 25. It can be seen in these figures that the agreement between the experiments and theory is excellent with the exception of the uncertainy of the Gas Analyzer for concentration below 1 percent, as pointed out by the supplier of the instrument.

[26] W. M. Kays, "Convective Heat and Mass Transfer," McGraw-Hill, New York (1966).

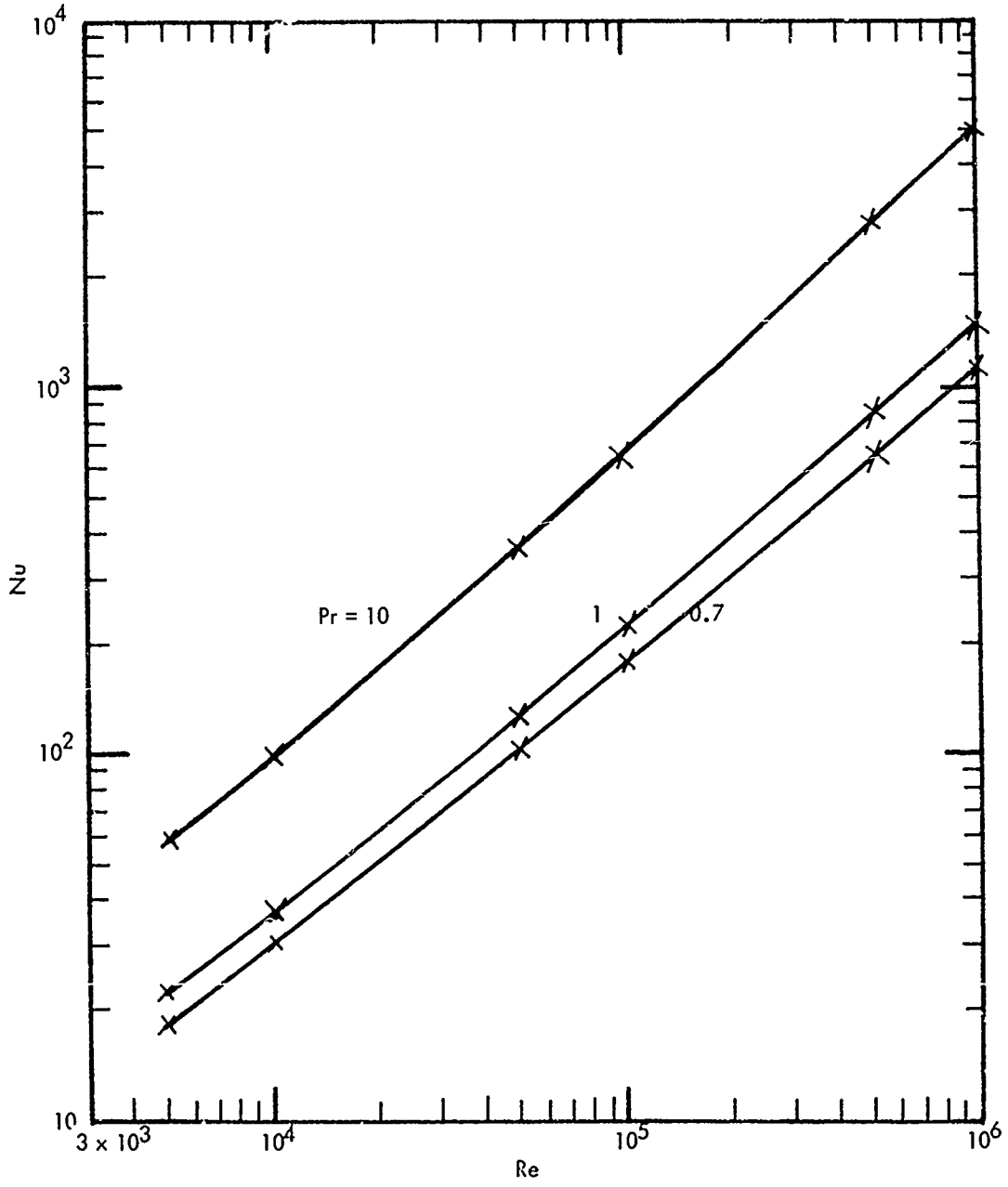

Fig. 20. Comparison of Nusselt number for fully developed turbulent flow with constant heat flux: —, Kays' correlation; X, present theory.

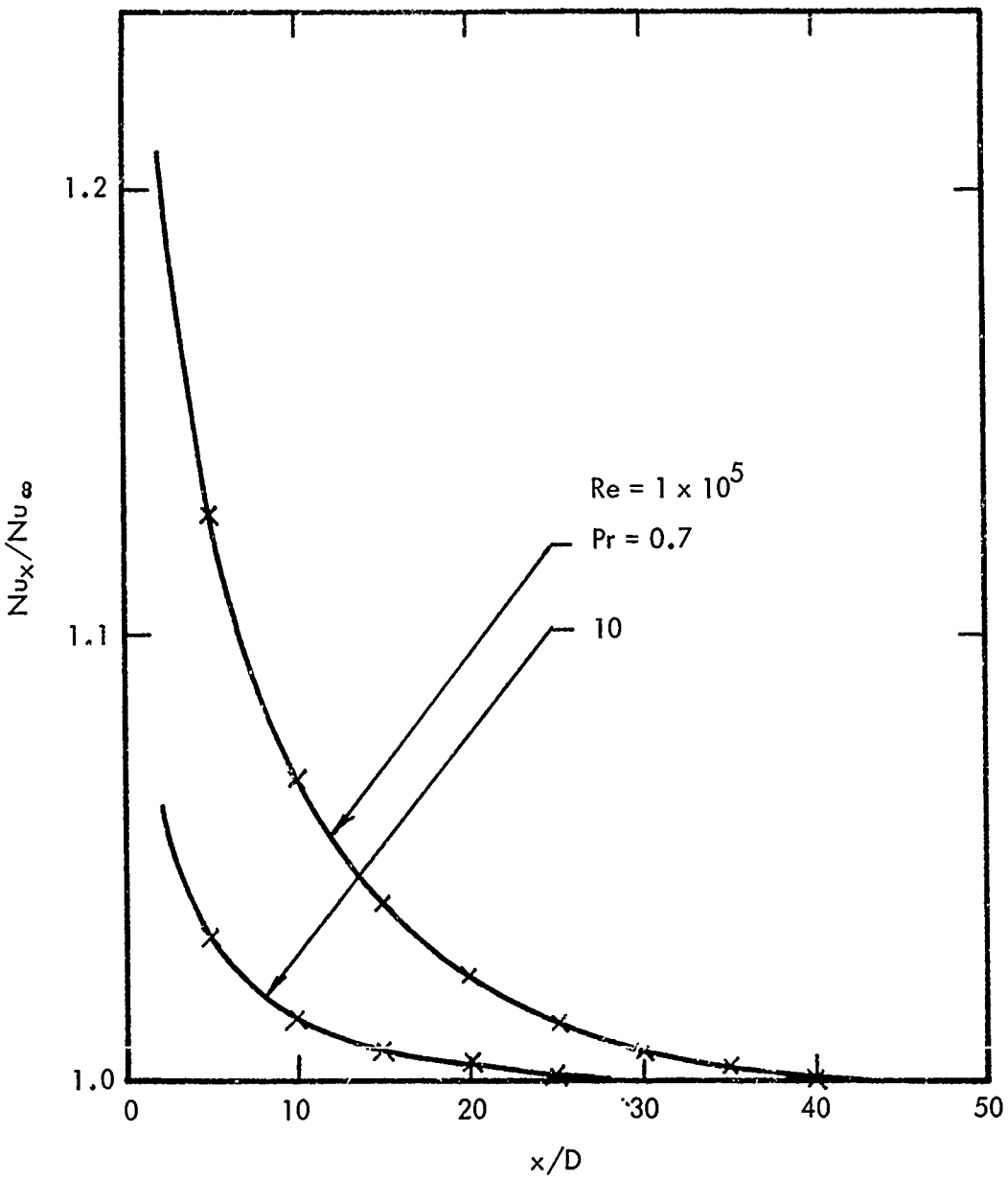

Fig. 21. Comparison of Nusselt number for turbulent flow with constant heat flux. —, Kays' correlation; X, present theory.

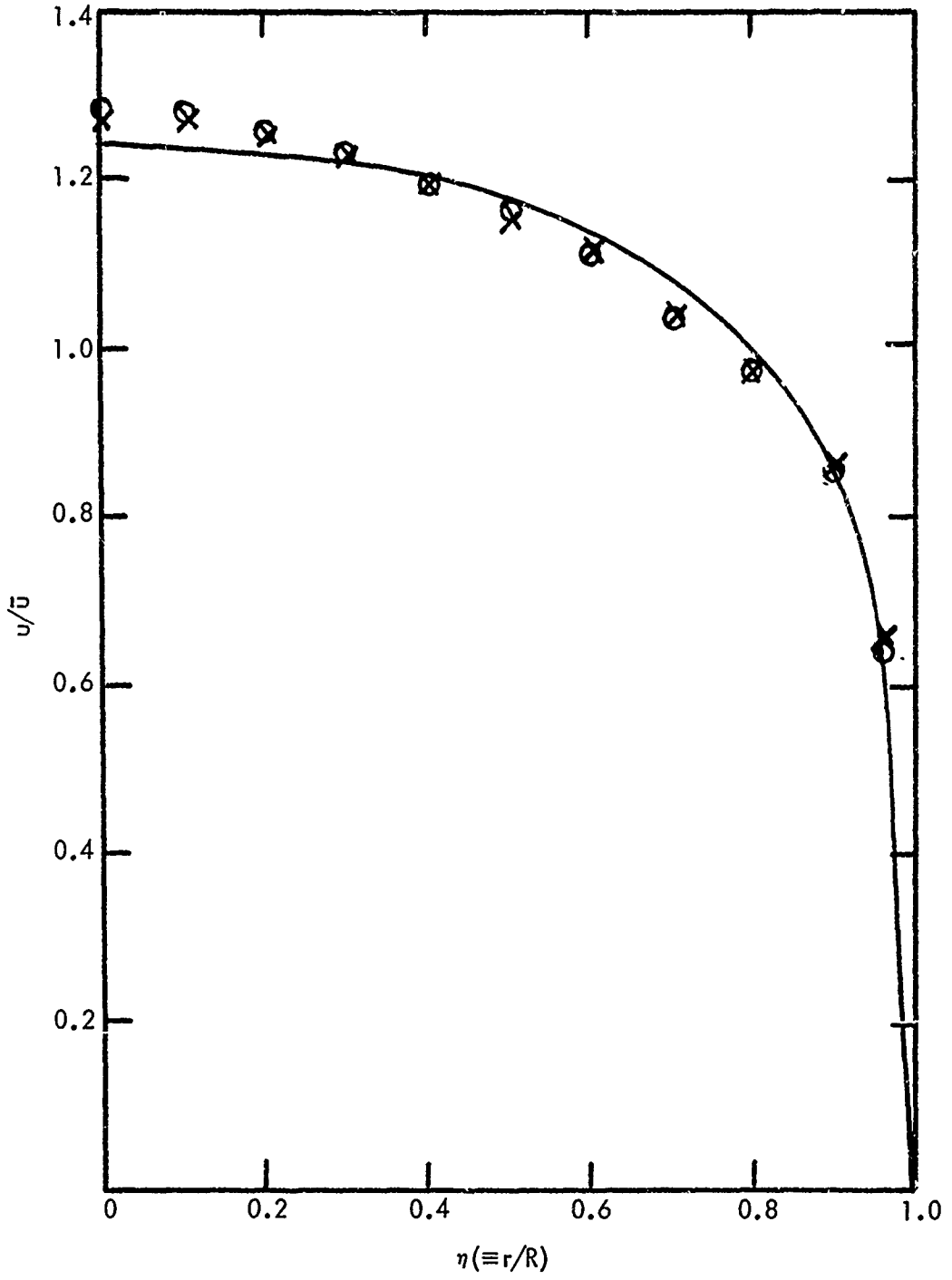

Fig. 22. Comparison of calculated and measured velocity profiles at Re = 1.5 x 10^4: —, present theory; X, experiments at $\bar{m}$ = 0; O, experiments at $\bar{m}$ = -0.0004.

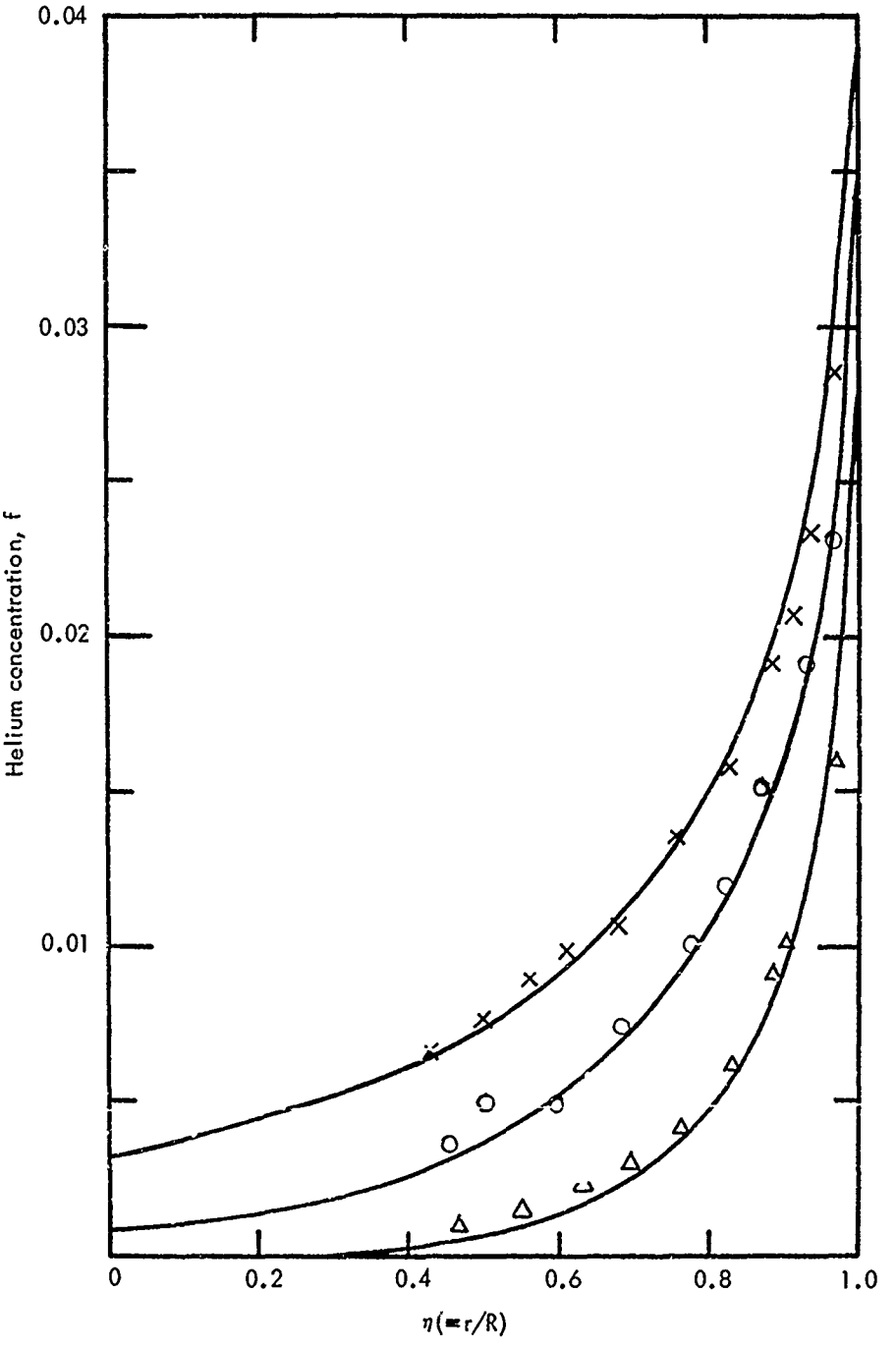

Fig. 23. Comparison of calculated and measured helium concentration at Re = 1.5 x 10^4 and $\overline{m}$ = -0.0002: — , present theory; X, O and Δ, experiments at x/D = 15, 10, and 5.

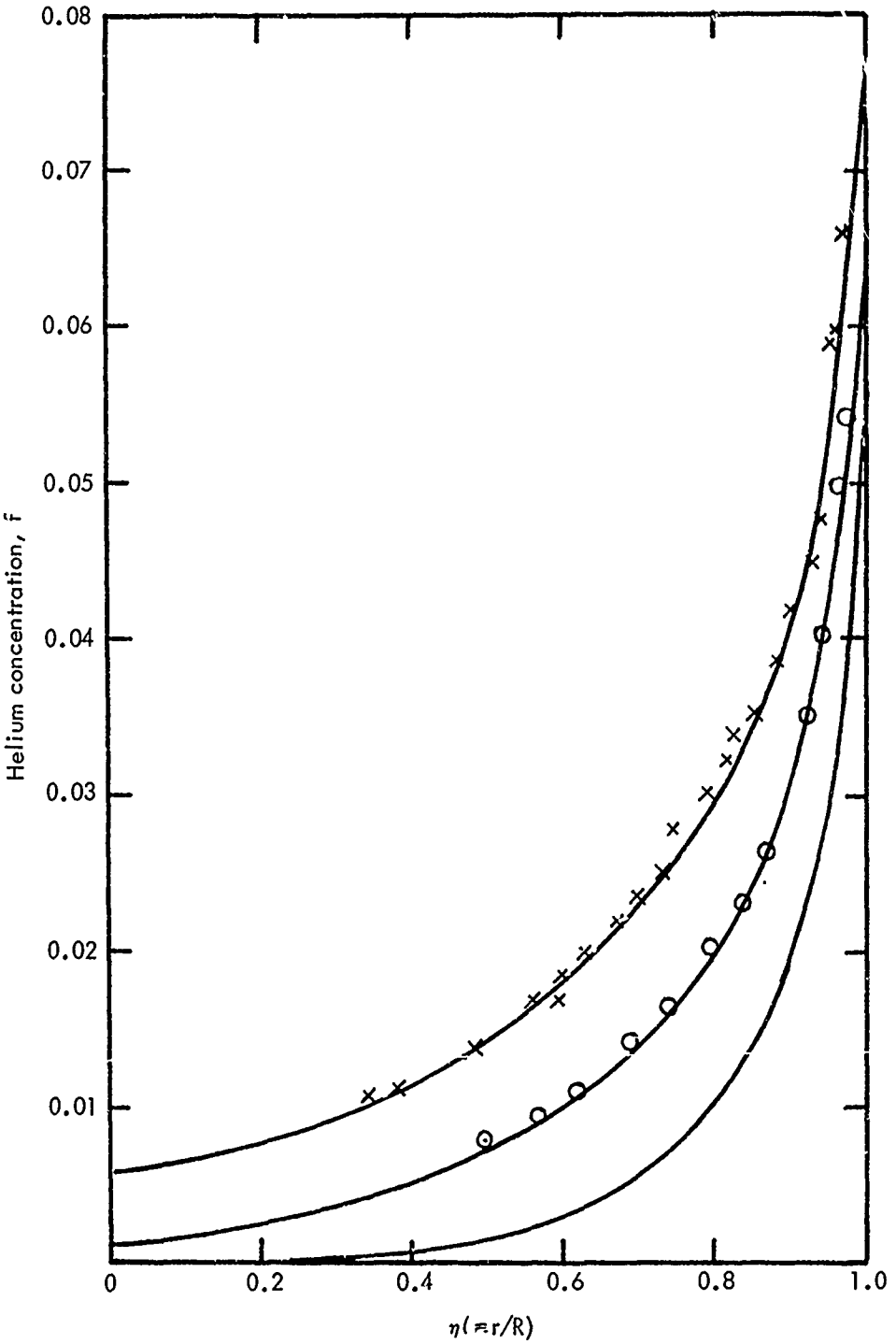

Fig. 24. Comparison of calculated and measured helium concentration at Re = 1.5 x 10^4 and $\overline{m}$ = -0.0004: —, present theory; X and O, experiments at x/D = 15 and 10.

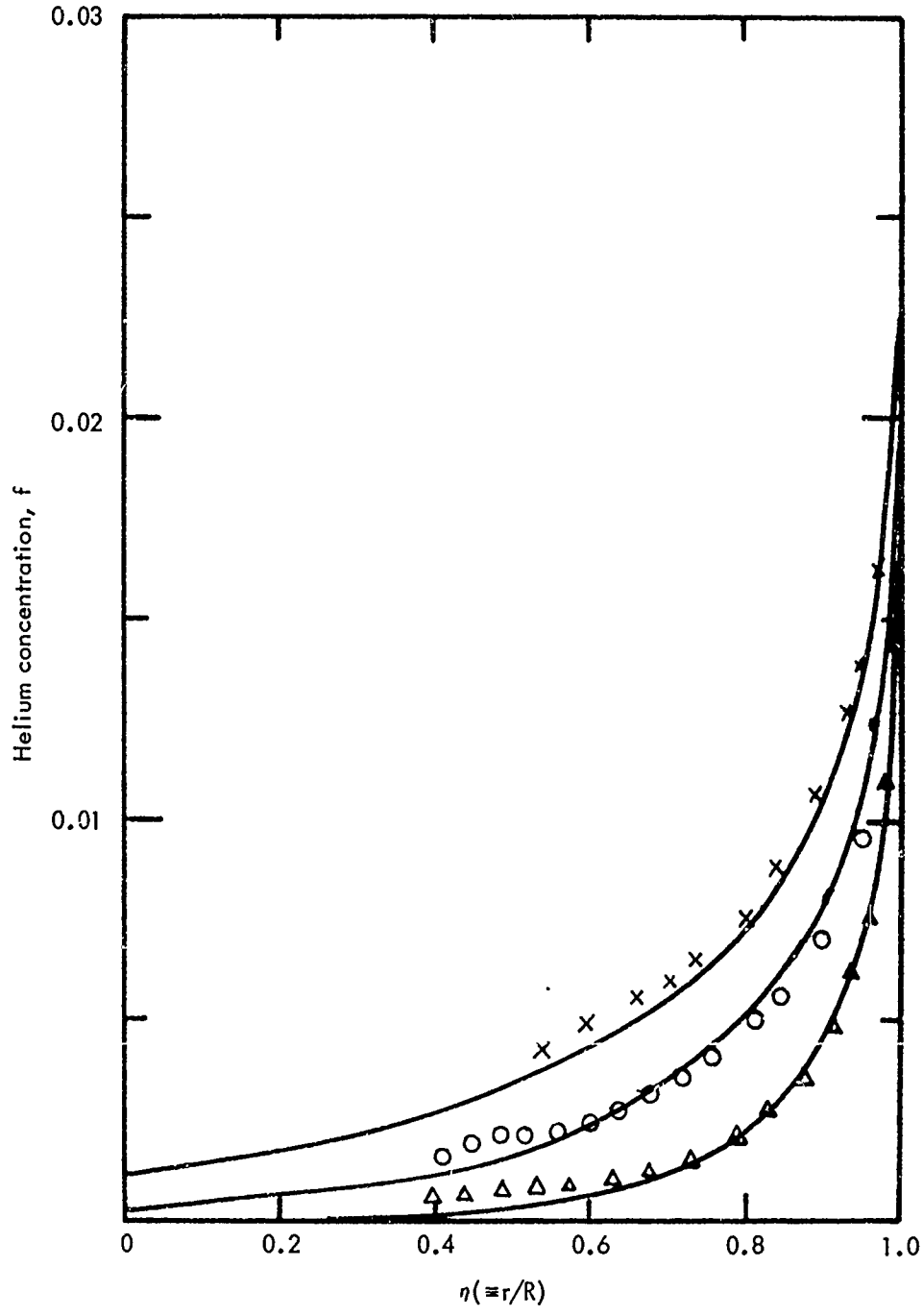

Fig. 25. Comparison of calculated and measured helium concentration at Re = 3 x 10^4 and $\overline{m}$ = -0.0001: —, present theory; X, O and Δ, experiments at x/D = 15, 10, and 5.

V. CONCLUSIONS

12. **Conclusions.** The results of this research can be summarized as follows:

a. A method for measurement of species concentration in a turbulent stream has been developed. The method has been applied to the measurement of helium concentration in air.

b. A theory has been developed for the solution of diffusion equations. A simplified assumption was made for the turbulent velocity profile. (The validity of this assumption for $\bar{m}$ up to 0.0004 can be judged by reference to Fig. 22.)

c. The theory is simple and quick to use in engineering calculations because the simultaneous solution of partial differential equations for conservation of mass, momentum, and species is replaced by the solution of a single partial differential equation for conservation of species.

d. The accuracy of the present solution can be judged by inspection of Figs. 18 through 21 and 23 through 25, where the present predictions are compared with available theoretical predictions and the present experiments.

e. The present method is restricted to the small wall-mass injection. This restriction, however, does not prevent its usefulness in a vast number of engineering applications.

f. In the reverse osmosis desalination of saline water, the wall-mass flux is usually small and so the present theory is applicable with slight modification of boundary condition (Equations (2) through (5)). Thus, the present theory should be used for optimization of the reverse osmosis process.

g. In the use of a catalytic converter for control of pollutant emission, the net wall-mass flux is zero and so present theory is again applicable. However, the reaction rate at the converter surface will determine the boundary condition for this problem. The present theory can be used to predict diffusion of pollutants in the gas stream, and subsequently performance of the converter can be calculated.

h. In application to the water supply system where dissolution of minerals and its salt must be predicted, the present theory should be used to calculate the water quality.

i. In some engineering devices, for example gas turbine combustors and diffusers, the wall-mass injection is large. Under such circumstances, the present theory

should be extended to the region of large wall-mass injection. The conservation equations for continuity of mass, momentum, and species will have to be solved simultaneously. In view of the fact that the momentum and diffusion equations are both parabolic, the present method can readily be extended to the problems with large wall-mass injection.

APPENDIX A

ENTRANCE VELOCITY PROFILE, $\phi_o(\eta)$

To derive the expression for velocity profile at the entrance to a porous tube, $\phi_o(\eta)$, analyses begin with the differential equation

$$-\mu_e \, (du/dr) \, / \, \tau_w = \tau/\tau_w = \eta \, . \tag{A1}$$

In this equation, the effective viscosity for turbulent flow, μ_e, is defined as the sum of the laminar and turbulent viscosities, μ and μ_t:

$$\mu_e = \mu + \mu_t \, . \tag{A2}$$

Among the various candidate representations for the turbulent viscosity, a model involving Prandtl's mixing length and Van Driest's damping factor has gained broad acceptance in recent years.[27 - 32]

This approach is employed here and gives the following model for the turbulent viscosity:

$$\mu_t = \rho l^2 / \partial u/\partial r/ \tag{A3}$$

$$1/R = DF \, (0.14 - 0.08\eta^2 - 0.06\eta^4) \tag{A4}$$

$$DF = 1\text{-}\exp \, [\, -R\sqrt{\tau_w/\rho} \, \, (1-\eta)/A\nu] \, . \tag{A5}$$

---

[27] R. B. Kinney and E. M. Sparrow, "Turbulent Flow, Heat Transfer, and Mass Transfer in a Tube with Surface Suction," ASME Paper No. 69-HT-4 (1969).

[28] E. M. Sparrow, V. K. Jonsson, G. S. Beavers, and R. G. Over, "Incompressible Turbulent Flow in a Permeable Wall Duct," ASME Paper No. 71-WA/FE-1 (1971).

[29] T. Cebeci, A. M. O. Smith, and G. Mosinskis, "Solution of the Incompressible Turbulent Boundary–Layer Equations," *J. Heat Transfer*, Vol. 92, pp. 133-143 (1970).

[30] S. V. Patankar and D. B. Spalding, "Heat and Mass Transfer in Boundary Layers," Morgan and Grampin, London (1967).

[31] S. W. Chi and C. C. Chang, "Effective Viscosity in a Turbulent Boundary Layer," *AIAA Journal*, Vol. 7, pp. 2032-2035 (1969).

[32] W. J. Glowacki and S. W. Chi, "Effect of Pressure Gradient on Mixing Length for Equilibrium Turbulent Boundary Layers," AIAA paper No. 72-213 (1972).

Equation (A3) expresses Prandtl's mixing length concept, while Equation (A4) is a representation for the mixing length, l, deduced by Nikuradse[33] from measured velocity profiles for the circular tube. Van Driest's damping factor[34] for an impermeable wall is expressed by Equation (A5). The quantity A is the damping constant which is equal to 26.

The effective viscosity expressions of Equations (A2) through (A5) may now be substituted into Equation (A1) yielding the following governing equation for the non-dimensional axial velocity, $u^+ (= \rho u \sqrt{\tau/\rho}/\mu)$:

$$\eta = -(1/R^+)(du^+/d\eta) + \left\{(0.14-0.08\eta^2-0.06\eta^4)\right.$$
$$\left.[1-\exp(-R^+(1-\eta)/A)]\right\}^2 (du^+/d\eta)^2 . \qquad (A6)$$

Integration of Equation (A6) with the boundary condition $u^+(R^+) = 0$ followed by considerable rearrangement gives the following expression for the axial velocity distribution:

$$u^+ = \int_\eta^1 2R^+\eta \left\{1 + [1+4\eta(R^+)^2 \left\{(0.14-0.08\eta^2-0.06\eta^4)\right.\right.$$
$$\left.\left.(1-\exp(-R^+(1-\eta)/A)\right\}^2]^{1/2}\right\}^{-1} d\eta . \qquad (A7)$$

In addition, the following relations can be verified in a straightforward manner:

$$\bar{u}_0^+ = 2\int_0^1 \eta u^+ d\eta \qquad (A8)$$

$$Re = 2R^+ u_0^+ \qquad (A9)$$

$$\phi_0 = u^+/\bar{u}_0^+ \qquad (A10)$$

Using Equations (A7) through (A9), $\phi_0(\eta)$ at different Re values and Re versus R^+ relation can be evaluated.

---

[33] H. Schlichting, "Boundary Layer Theory," McGraw-Hill, New York (1968).

[34] E. R. Van Driest, "On Turbulent Flow Near a Wall," *J. Aero. Sci.*, Vol. 23, pp. 1006-1011, 1036 (1956).

APPENDIX B

LISTING AND USERS' INSTRUCTION OF COMPUTER PROGRAM

FOR TURBULENT DIFFUSION IN ROUND TUBES

A computer program for calculation of turbulent diffusion in round tubes has been written in Fortran IV language. The program has been checked out on CDC 6000 series and IBM 360 series computers. A complete listing of the computer program is presented below, and main FORTRAN input and output symbols are defined. All the input integers, beginning with L through N, are 5-digit figures (I5), and all other input constant are 15-digit figures (E15.6).

Input Symbols:

TSTA	a constant to suppress underflow 1×10^{-25}
TSTF	a constant to suppress underflow 1×10^{-25}
NRPS	number of nondimensional radius R^+
RPS	nondimensional radius, R^+
SC	Schmidt number
SCT	turbulent Schmidt number
NZETA	number of increment in axial direction
DDZT	initial increment in axial direction, $\delta\xi$, 1×10^{-6}
NMBAR	number of nondimensional wall-mass injection rate
AMBAR	nondimensional wall-mass injection rate, $\overline{m}$

Output Symbols:

RE	Reynolds number at entrance to diffusion section
ETA	nondimensional radius, η
DU/DETA	nondimensional gradient of velocity $d\phi_0/d\eta$
U/UB	nondimensional axial velocity defined as local velocity divided by bulk average velocity, ϕ_o
U/UC	nondimensional axial velocity defined as local velocity divided by center-line velocity
SC	Schmidt number
SCT	turbulent Schmidt number
MB	nondimensional wall-mass injection rate, $\bar{m}$
ZETA	nondimensional axial position, ξ (= χ/R)
F	mass concentration of species under consideration, f
FBAR	species concentration defined as $(f_\omega - f)/(f_\omega - \dot{f})$
FCB	species concentration defined as $(f-f_\phi)/(f_w-f_\phi)$
Nu	Nusselt number

```
      PROGRAM MAIN    (INPUT,OUTPUT,TAPE5=INPUT,TAPE6=OUTPUT)
C TURBULENT DIFFUSION IN ROUND TUBES
      DIMENSION ETA(241), UO(241), V(241), F(241), A(241), B(241),
     1U1(241), U2(241), DUO(241), EDE1(241), EDE2(241)
      WRITE (6,21)
      READ (5,12) TSTA, TSTF
      READ (5,1) NRPS
      DO 101 NR=1,NRPS
      READ (5,11) RPS
      ETA(1)=0.
      UO(1)=0.
      DUO(1)=0.
    1 FORMAT (I5)
   11 FORMAT (E15.6)
   12 FORMAT (2E15.6)
   13 FORMAT (3E15.6)
   14 FORMAT (4E15.6)
   21 FORMAT (//35H TURBULENT DIFFUSION IN ROUND TUBES)
   22 FORMAT (/4H RE=,E15.6)
   23 FORMAT (/53H      ETA          DU/DETA          U/UB          U/UC)
   24 FORMAT (/53H       RE            SC             SCT            MB)
   25 FORMAT (/6H ZETA=,E15.6)
   26 FORMAT (/53H      ETA            F            FBAR           FCB)
   27 FORMAT (/5H  NU=,E15.6)
      I=1
      J=0
      N=1
      DO 102 IN=1,8
      IF (N-1) 211,201,211
  211 IF (N-2) 212,202,212
  212 IF (N-3) 213,203,213
  213 IF (N-4) 214,204,214
  214 IF (N-5) 215,205,215
  215 IF (N-6) 216,206,216
  216 IF (N-7) 217,207,217
  217 IF (N-8) 218,208,218
  218 CONTINUE
  201 DETA=0.0064
      M=40
      GO TO 220
  202 DETA=0.0032
      M=40
      GO TO 220
  203 DETA=0.0016
      M=40
      GO TO 220
  204 DETA=0.0008
      M=40
      GO TO 220
  205 DETA=0.0004
      M=40
      GO TO 220
  206 DETA=0.0002
      M=10
      GO TO 220
  207 DETA=0.0001
      M=10
      GO TO 220
  208 DETA=0.00005
      M=20
      GO TO 220
  220 DO 103 K=1,M
```

```
      J=J+1
      I=I+1
      IF (K-1) 222,223,22
  223 IF (N-1) 222,224,22
  224 E1=0.0064
      E2=0.0128
      ETA(I)=0.012
      GO TO 225
  222 E1=ETA(J)+DETA
      E2=E1+DETA
      ETA(I)=E2
  225 DU1=2.*RPS*E1/(1.+SQRT(1.+4.*E1*RPS*RPS*(0.14-0.080*E1**2-0.06
     1*E1**4)**2*(1.-EXP((-1.*RPS*(1-E1))/26.))**2))
      DU2=2.*RPS*E2/(1.+SQRT(1.+4.*E2*RPS*RPS*(0.14-0.080*E2**2-0.06
     1*E2**4)**2*(1.-EXP((-1.*RPS*(1-E2))/26.))**2))
      DUO(I)=DU2
      UO(I)=DETA*(DUO(J)+4.*DU1+DU2)/3.
      UO(I)=UO(J)+UO(I)
  103 CONTINUE
      N=N+1
  102 CONTINUE
      DO 104 I=1,24
      K=I-1
      UO(I)=UO(241)-UO(I)
      J=I+1
      IF (I-1) 105,106,105
  106 UB=0.
      GO TO 104
  105 CONTINUE
  107 UB=UB+(ETA(I)*UO(I)+ETA(K)*UO(K))*(ETA(I)-ETA(K))
  104 CONTINUE
      RE=UB*RPS
      REW=2.*RE
      J=9
      WRITE (6,22) REW
      WRITE (6,23)
      DO 108 I=1,241
      J=J+1
      UO(I)=UO(I)/UB
      DUO(I)=DUO(I)/UB
      UUC=UO(I)/UO(1)
      IF (J-10) 108,110,108
  110 WRITE (6,14) ETA(I),DUO(I),UO(I),UUC
      J=0
  108 CONTINUE
      READ (5,13) SC,SCT
      READ (5,1) NZETA
      READ (5,11) DDZT
      READ (5,1) NMBAR
      ZETA=0
      DO 500 IMB=1,NMBAR
      READ (5,11) AMBAR
      WRITE (6,24)
      REW=2.*RE
      WRITE (6,14)REW,SC,SCT,AMBAR
      ZETA=0.
      DZETA=DDZT
      DO 450 INZ=1,NZETA
      IF (INZ-23) 871,871,872
  871 DZETA=2.*DZETA
      GO TO 873
  872 DZETA=0.5
  873 CONTINUE
      IF (INZ-1) 451,452,451
  452 CONTINUE
      DO 440 K=1,241
```

```
      F(K)=0
      IF (K-1) 456,457,456
  457 V(K)=0.
      VB=0.
      VVK=0.
      GO TO 611
  456 KA=K-1
      VC=RE*AMBAR*UO(K)*ETA(K)
      VVK =VVK  +(VB+VC)*(ETA(K)-ETA(KA))
      V(K)=VVK/ETA(K)
      VB=VC
  611 CONTINUE
      U1(K)=UO(K)*RE
      AKI=AMBAR*RE*(1.-ETA(K))/2
      DF=SQRT(AKI**4+4.*(RPS*(1.-ETA(K))/26.)**4)
      DF=SQRT(DF+AKI**2)/(SQRT(2.))
      DF=1-EXP(-AKI-DF)
      IF (K-1) 613,612,613
  613 CONTINUE
      EDE1(K)=DF*(0.14-0.08*ETA(K)**2-0.06*ETA(K)**4)
      EDE1(K)=RE*DUO(K)*EDE1(K)**2/SCT
      EDE1(K)=1./SC+EDE1(K)
      EDE1(K)=ETA(K)*EDE1(K)
      GO TO 440
  612 EDE1(K)=0.
  440 CONTINUE
      GO TO 454
  451 DO 453 K=1,241
      U1(K)=U2(K)
      EDE1(K)=EDE2(K)
  453 CONTINUE
  454 ZETA1=ZETA
      ZETA=ZETA+DZETA
      DO 455 K=1,241
      U2(K)=RE*(1.-2.*AMBAR*ZETA)*UO(K)
      IF (K-1) 614,615,614
  614 CONTINUE
      EDE2(K)=EDE1(K)/ETA(K)-1./SC
      EDE2(K)=EDE2(K)*(1.-2.*AMBAR*ZETA)/(1.-2.*AMBAR*ZETA1)
      EDE2(K)=(EDE2(K)+1./SC)*ETA(K)
      GO TO 455
  615 EDE2(K)=0.
  455 CONTINUE
      DO 301 IN=1,8
      IF(IN-1) 411,401,411
  411 IF(IN-2) 412,402,412
  412 IF(IN-3) 413,403,413
  413 IF(IN-4) 414,404,414
  414 IF(IN-5) 415,405,415
  415 IF(IN-6) 416,406,416
  416 IF(IN-7) 417,407,417
  417 IF(IN-8) 418,408,418
  418 CONTINUE
  401 DETA=0.0128
      M=40
      GO TO 420
  402 DETA=0.0064
      M=40
      GO TO 420
  403 DETA=0.0032
      M=40
      GO TO 420
  404 DETA=0.0016
      M=40
      GO TO 420
  405 DETA=0.0008
```

```
      M=40
      GO TO 420
  406 DETA=0.0004
      M=10
      GO TO 420
  407 DETA=0.0002
      M=10
      GO TO 420
  408 DETA=0.0001
      M=20
  420 IF (IN-1) 431,430,431
  430 BETA=0.5*(U1(1)+U2(1))/DZETA+2./(SC*DETA*DETA)
      GAMA=-2./(SC*DETA*DETA)
      DELT=0.5*(U1(1)+U2(1))/DZETA-2./(SC*DETA*DETA)
      DELT=DELT*F(1)+2.*F(2)/(SC*DETA*DETA)
      A(1)=-GAMA/BETA
      B(1)=DELT/BETA
      I=0
      MM=0
  431 DO 441 K=1,M
      I=I+1
      J=I+1
      L=J+1
      IF (K-M) 433,436,433
  436 IF (IN-8)437,434,437
  437 L=L+1
  433 ED1=0.25*(EDE1(I)+EDE1(J)+EDE2(I)+EDE2(J))
      ED2=0.25*(EDE1(J)+EDE1(L)+EDE2(J)+EDE2(L))
      UU=0.5*(U1(J)+U2(J))
      VV=0.5*(V(J)+V(J))
      ALFA=-0.5*ED1/(ETA(J)*DETA*DETA)-0.25*VV/DETA
      BETA=UU/DZETA+0.5*(ED1+ED2)/(ETA(J)*DETA*DETA)
      GAMA=0.25*VV/DETA-0.5*ED2/(ETA(J)*DETA*DETA)
      DELT=F(I)*(0.5*ED1/(ETA(J)*DETA*DETA)+0.25*VV/DETA)
     1+F(J)*(UU/DZETA-0.5*(ED1+ED2)/(ETA(J)*DETA*DETA))
     2+F(L)*(0.5*ED2/(ETA(J)*DETA*DETA)-0.25*VV/DETA)
      IF (L-J-1) 438,625,438
  625 IF (MM) 470,439,470
  439 A(J)=-GAMA /(ALFA*A(I)+BETA)
      B(J)=(DELT-ALFA*B(I))/(ALFA*A(I)+BETA)
      GO TO 441
  438 I=J
      J=J+1
      MM=31
      DETA=0.5*DETA
      ALFA1=ALFA
      BETA1=BETA
      GAMA1=GAMA
      DELT1=DELT
      GO TO 433
  470 MM=I-1
      A(I)=GAMA1*BETA/(GAMA*(ALFA1*A(MM)+BETA1)-GAMA1*ALFA)
      B(I)=(GAMA*(DELT1-ALFA1*B(MM))-GAMA1*DELT)/(GAMA*
     1(ALFA1*A(MM)+BETA1)-GAMA1*ALFA)
      I=MM
      MM=0
      GO TO 441
  434 AAM=DETA*RE*SC*AMBAR
      BETA=BETA+GAMA/(1.-AAM)
      DELT=DELT+AAM*GAMA/(1.-AAM)
      II=I-1
      F(I)=(DELT-ALFA*B(II))/(ALFA*A(II)+BETA)
      F(J)=(F(I)-AAM)/(1.-AAM)
  441 CONTINUE
  301 CONTINUE
      DO 474 K=1,230
```

```
      I=240-K
      J=I+1
      IF (ABS(A(I))-TSTA) 701,702,702
  702 IF (ABS(F(J))-TSTF) 701,703,703
  703 F(I)=A(I)*F(J)+B(I)
      GO TO 474
  701 F(I)=B(I)
  474 CONTINUE
      WRITE (6,25) ZETA
      FR=F(241)
      FB=-2.*ZETA*AMBAR/(1.-2.*ZETA*AMBAR)
      RNU=(FR-F(240))/(DETA*(FR-FB))
      RNU=2.*RNU
      WRITE (6,27) RNU
      WRITE (6,26)
      DO 475 I=1,241,10
      FBAR=(FR-F(I))/(FR-FB)
      FCB=(F(I)-F(241))/(F(1)-F(241))
      WRITE (6,14) ETA(I),F(I),FBAR,FCB
  475 CONTINUE
  450 CONTINUE
      DZETA=DDZT
  500 CONTINUE
  101 CONTINUE
      CALL EXIT
      STOP
      END
```

```
  06/26/72  SCOPE 3.3R1          MERDC MAY  05/01/72
14.10.46.MTAP332
14.10.46.MTAP3,CM60000,T400.  PATIL
14.10.47.TASK(TNMT72039,PW******,TRTS,SCIR)
14.10.47.COPYCF(INPUT,X)
14.10.48.REWIND(X)
14.10.48.COPYSBF(X,OUTPUT)
14.10.49.CP     000.033 SEC.
14.10.49.PP     001.390 SEC.
14.10.49.IO     000.081 SEC.
```